HEATING EFFECT OF ELECTROMAGNETIC FIELDS ON HUMAN HEAD AT GSM FREQUENCIES

A THESIS SUBMITTED TO
THE GRADUATE SCHOOL OF NATURAL AND APPLIED SCIENCES
OF
ÇANKAYA UNIVERSITY

BY

AFŞAR TÜRK

IN PARTIAL FULLFILMENT OF THE REQUIREMENTS
FOR
THE DEGREE OF MASTER OF SCIENCE
IN
ELECTRONIC AND COMMUNICATION ENGINEERING

SEPTEMBER 2010

Title of the Thesis : **Heating Effect of Electromagnetic Fields on Human Head at GSM Frequencies**

Submitted by **Afşar TÜRK**

Approval of the Graduate School of Natural and Applied Sciences, Çankaya University

Prof. Dr. Taner ALTUNOK
Director

I certify that this thesis satisfies all the requirements as a thesis for the degree of Master of Science.

Assoc. Prof. Dr. Celal Zaim ÇİL
Head of Department

This is to certify that we have read this thesis and that in our opinion it is fully adequate, in scope and quality, as a thesis for the degree of Master of Science.

Assoc. Prof. Dr. Cem ÖZDOĞAN
Co-Supervisor

Prof. Dr. Yahya Kemal BAYKAL
Supervisor

Examination Date : 02.09.2010

Examining Committee Members :

Prof. Dr. Yahya Kemal BAYKAL (Çankaya Univ.)

Prof. Dr. Erdem YAZGAN (Hacettepe Univ.)

Asist. Prof. Dr. Serap ALTAY ARPALI (Çankaya Univ.)

STATEMENT OF NON-PLAGIARISM

I hereby declare that all information in this document has been obtained and presented in accordance with academic rules and ethical conduct. I also declare that, as required by these rules and conduct, I have fully cited and referenced all material and results that are not original to this work.

Name, Last Name	: Afşar TÜRK
Signature	: 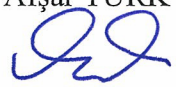
Date	: 02.09.2010

ABSTRACT

HEATING EFFECT OF ELECTROMAGNETIC FIELDS ON HUMAN HEAD AT GSM FREQUENCIES

TÜRK, Afşar

M.Sc., Department of Electronics and Communication Engineering

Supervisor: Prof. Dr. Yahya Kemal BAYKAL

Co-supervisor: Assoc. Prof. Dr. Cem ÖZDOĞAN

September 2010, 35 pages

This thesis investigates the heating effect of electromagnetic fields on human head at GSM (Global System for Mobile Communications) frequencies. First of all, existing structure was studied. In this work, the existing spherical head models of head are searched and the head is modelled with different concentric spheres (brain, bone, skin) that have different permittivity and conductivity. The radiation is assumed to be generated by a loop antenna located near the head. The results are obtained at two different frequencies, 900 MHz and 1800 MHz that are widely used in GSM systems. To investigate relations between permittivity, conductivity and heating potential, the numerical results are found on any sphere that has different radius, permittivity and conductivity.

Keywords: Electromagnetic Fields, Biological Tissues, GSM.

ÖZ

GSM FREKANSLARINDAKİ ELEKTROMANYETİK ALANLARIN İNSAN KAFASI ÜZERİNDEKİ ISI ETKİSİ

TÜRK, Afşar

Yüksek Lisans, Elektronik ve Haberleşme Mühendisliği Anabilim Dalı

Tez Yöneticisi: Prof. Dr. Yahya Kemal BAYKAL

Ortak Tez Yöneticisi: Doç. Dr. Cem ÖZDOĞAN

Eylül 2010, 35 sayfa

Bu tez GSM frekanslarındaki elektromanyetik alanların insan kafası üzerindeki ısı etkisini araştırmaktadır. Öncelikle mevcut yapı çalışıldı. Bu çalışmada, mevcut küresel kafa modelleri araştırıldı ve kafa farklı dielektrik sabit ve iletkenliğe sahip farklı ortak merkezli kürelerle (beyin, kemik, deri) modellendi. Işımanın kafanın yanına yerleştirilmiş döngüsel bir anten tarafından üretildiği kabul edildi. Sonuçlar GSM sistemlerinde geniş ölçüde kullanılan 900 MHz ve 1800 MHz gibi iki farklı frekansta elde edildi. Dielektrik sabiti, iletkenlik ve ısı potansiyeli arasındaki ilişkileri araştırmak için farklı yarıçap, dielektrik sabiti ve iletkenliğe sahip bir küre üzerinde nümerik sonuçlar bulundu.

Anahtar Kelimeler: Elektromanyetik Alanlar, Biyolojik Dokular, GSM.

ACKNOWLEDGEMENTS

The author wishes to express his special thanks to his supervisor Prof. Dr. Yahya Kemal BAYKAL and co-supervisor Assoc. Prof. Dr. Cem ÖZDOĞAN for their support, guidance, advice throughout this thesis study.

The author would also like to thank his family for their great encouragement and support.

TABLE OF CONTENTS

STATEMENT OF NON-PLAGIARISM iii
ABSTRACT iv
ÖZ.....v
ACKNOWLEDGEMENTS vi
TABLE OF CONTENTS.....vii
LIST OF TABLES.....ix
LIST OF FIGURES x
LIST OF ABBREVIATIONS xii
CHAPTERS:
1. INTRODUCTION 1
2. METHOD.....6
2.1 The Theory of State-Space Formulation of Scattering.....6
2.1.1 The formulation of scattering from inhomogeneous dielectric spherical shells.....7
2.2 Extension of the Theory to Structures with Homogenous Dielectric Core. 8
2.2.1 General description of the problem.....8
3. THE DISTRIBUTION OF THE HEATING POTENTIAL IN THE HEAD MODEL.....11
4. RELATION BETWEEN PERMITTIVITY, CONDUCTIVITY AND HEATING POTENTIAL 21
5. CONCLUSION.....34
REFERENCES R1
APPENDICESY:
APPENDIX A..... A1
A.1 Calculation of SAR..... A1

A.2 Electric Field of Loop Antenna A2
APPENDIX B…….. ..... A3
B.1 Limit Values in Turkey A3
B.2 SAR Values of Cell Phones A4
APPENDIX C…….. ..... A5
CURRICULUM VITAE A5

LIST OF TABLES

Table 2.1: Complex Dielectric Specifications of the Head Model That Is Used in Simulation 10

Table 3.1: FCC Limits for Localized (Partial-body) Exposure 16

Table 3.2: For R_{12}=10 *cm* Absorbed Max. Power, SAR Values 16

Table 3.3: For R_{12}=12 *cm* Absorbed Max. Power, SAR Values 16

Table 3.4: For R_{12}=14 *cm* Absorbed Max. Power, SAR Values 17

Table 3.5: For R_{12}=16 *cm* Absorbed Max. Power, SAR Values 17

Table 3.6: For R_{12}=10 *cm* Absorbed Max. Power, SAR Values 20

Table 3.7: For R_{12}=16 *cm* Absorbed Max. Power, SAR Values 20

Table 4.1: For ε_r = 10, σ = 100, R_{12}=2 *cm*, Absorbed Max. Power Values 32

Table 4.2: For ε_r = 10, σ = 2000, R_{12}=2 *cm*, Absorbed Max. Power Values 32

Table 4.3: For ε_r = 100, σ =100, R_{12}=2 *cm*, Absorbed Max. Power Values 32

Table 4.4: For ε_r = 100, σ =2000, R_{12}=2 *cm*, Absorbed Max. Power Values 32

Table 4.5: For ε_r = 10, σ = 100, R_{12}=3 *cm*, Absorbed Max. Power Values 33

Table 4.6: For ε_r = 10, σ = 2000, R_{12}=3 *cm*, Absorbed Max. Power Values 33

Table 4.7: For ε_r = 100, σ =100, R_{12}=3 *cm*, Absorbed Max. Power Values 33

Table 4.8: For ε_r = 100, σ =2000, R_{12}=3 *cm*, Absorbed Max. Power Values 33

Table B.1.1: Limit Values for Uncontrolled Exposure in Turkey A3

Table B.1.2: Limit Values for Controlled Exposure A3

Table B.2.1: The Ten Highest Radiating Cell Phones (Europe) A4

Table B.2.2: The Ten Lowest Radiating Cell Phones (Europe) A4

LIST OF FIGURES

Figure 1.1: The Electromagnetic Spectrum 2
Figure 2.1: Block Diagram of Scattering 7
Figure 2.2: Spherical Head Model and Configuration.....9
Figure 3.1: Heating Potential at f = 900 *MHz*, R_{12}=10 *cm*, ka_1=0,3.....11
Figure 3.2: Heating Potential at f = 900 *MHz*, R_{12}=12 *cm*, ka_1=0,3.....12
Figure 3.3: Heating Potential at f = 900 *MHz*, R_{12}=14 *cm*, ka_1=0,3.....12
Figure 3.4: Heating Potential at f = 900 *MHz*, R_{12}=16 *cm*, ka_1=0,3.....13
Figure 3.5: Heating Potential at f = 1800 *MHz*, R_{12}=10 *cm*, ka_1=0,3.....13
Figure 3.6: Heating Potential at f = 1800 *MHz*, R_{12}=12 *cm*, ka_1=0,3.....14
Figure 3.7: Heating Potential at f = 1800 *MHz*, R_{12}=14 *cm*, ka_1=0,3.....14
Figure 3.8: Heating Potential at f = 1800 *MHz*, R_{12}=16 *cm*, ka_1=0,3.....15
Figure 3.9: Heating Potential at f = 900 *MHz*, R_{12}=10 *cm*, a_1=1 *cm*.....18
Figure 3.10: Heating Potential at f = 900 *MHz*, R_{12}=16 *cm*, a_1=1 *cm*.....18
Figure 3.11: Heating Potential at f =1800 *MHz*, R_{12}=10 *cm*, a_1=1 *cm*.....19
Figure 3.12: Heating Potential at f =1800 *MHz*, R_{12}=16 *cm*, a_1=1 *cm*.....19
Figure 4.1: Heating Potential at f =900 *MHz*, R_{12}=2 *cm*, a_1=1 *cm*.....22
Figure 4.2: Heating Potential at f =1800 *MHz*, R_{12}=2 *cm*, a_1=1 *cm*.....22
Figure 4.3: Heating Potential at f =900 *MHz*, R_{12}=2 *cm*, a_1=1 *cm*.....23
Figure 4.4: Heating Potential at f =1800 *MHz*, R_{12}=2 *cm*, a_1=1 *cm*.....23
Figure 4.5: Heating Potential at f =900 *MHz*, R_{12}=2 *cm*, a_1=1 *cm*.....24
Figure 4.6: Heating Potential at f =1800 *MHz*, R_{12}=2 *cm*, a_1=1 *cm*.....24
Figure 4.7: Heating Potential at f =900 *MHz*, R_{12}=2 *cm*, a_1=1 *cm*.....25
Figure 4.8: Heating Potential at f =1800 *MHz*, R_{12}=2 *cm*, a_1=1 *cm*.....25
Figure 4.9: Heating Potential at f =900 *MHz*, R_{12}=3 *cm*, a_1=1 *cm*.....26
Figure 4.10: Heating Potential at f =1800 *MHz*, R_{12}=3 *cm*, a_1=1 *cm*.....26
Figure 4.11: Heating Potential at f =900 *MHz*, R_{12}=3 *cm*, a_1=1 *cm*.....27

Figure 4.12: Heating Potential at f =1800 *MHz*, R_{12}=3 *cm*, a_1=1 *cm*.....27
Figure 4.13: Heating Potential at f =900 *MHz*, R_{12}=3 *cm*, a_1=1 *cm*.....28
Figure 4.14: Heating Potential at f =1800 *MHz*, R_{12}=3 *cm*, a_1=1 *cm*.....28
Figure 4.15: Heating Potential at f =900 *MHz*, R_{12}=3 *cm*, a_1=1 *cm*.....29
Figure 4.16: Heating Potential at f =1800 *MHz*, R_{12}=3 *cm*, a_1=1 *cm*.....29
Figure 4.17: Power Variation Versus σ , at ε_r = 10, f = 900 *MHz* 30
Figure 4.18: Power Variation Versus σ, at ε_r = 10, f = 1800 *MHz* 30
Figure 4.19: Power Variation Versus σ , at ε_r = 100, f = 900 *MHz* 31
Figure 4.20: Power Variation Versus σ , at ε_r = 100, f = 1800 *MHz*.....31
Figure A.2.1: Small Loop Antenna.....A2

LIST OF ABBREVIATIONS

DECT	Digital Enhanced Cordless Telecommunications
DNA	Deoxyribonucleic Acid
EEG	Electroencephalography
EM	Electromagnetic
EMF	Electromagnetic Fields
FCC	Federal Communications Commission
FDTD	Finite-Difference Time-Domain
GSM	Global System for Mobile Communications
ICNIRP	International Commission on Non-Ionazing Radiation Protection
MRI	Magnetic Resonance Imaging
RF	Radio Frequency
SAR	Specific Absorption Rate
WHO	World Health Organization

CHAPTER 1

INTRODUCTION

With the increase of telecommunication needs, a lot of different frequencies are being used in many different environments. Especially with the vast use of mobile phones, it becomes important to understand the effects of mobile system frequencies on living things. Especially in regions where the power of electromagnetic radiation is high, it is essential to understand how human body will be effected under such radiation. It is known that GSM system frequencies widely used all over the world that interact a lot with the human head.

In this work we investigate the heating effect of electromagnetic fields on human head at GSM frequencies of 900 MHz and 1800 MHz. Existing spherical head models were searched [1], [2], [3], [4], [5], [6], [7].

First of all, some general knowledge is given about electromagnetic exposure. The natural and man made sources emit electromagnetic fields. These sources are electrical discharges in the earth's atmosphere, radiation from sun/space, everyday use of devices and systems, medical devices/applications, communication systems and others.

In recent years specialized exposure systems have been designed for laboratory studies.

Important points about RF exposure of biological systems are modulation, incident electric-field and magnetic-field strengths, incident power density, source frequency, type and distance of exposure, and duration of exposure. These quantities are all

functions of its relationship to the physical configuration and dimension of the biological body.

Biological tissue heating is the most widely interaction mechanism of microwave radiation with biological systems. The effect can result from elevations of tissue temperature affected by RF energy absorbed in biological systems. The complex permittivity and electrical conductivity cause the electric fields to be absorbed in cells and tissues of human body. For partial body exposures, if the amount of RF energy absorbed is excessive rapid temperature rise and local tissue damage may occur. A temperature rise on the order of 1^{o} C in humans can result from an SAR input of $4\,W/kg$.

RF part of the electromagnetic spectrum is used for broadcasting and telecommunication. Electromagnetic fields in this frequency range have natural or man made origin. They may have a continuous sinusodial waveform, but more often they have a complex amplitude distribution over time [8]. FCC Limits for Localized (Partial-body) Exposure are provided in [9].

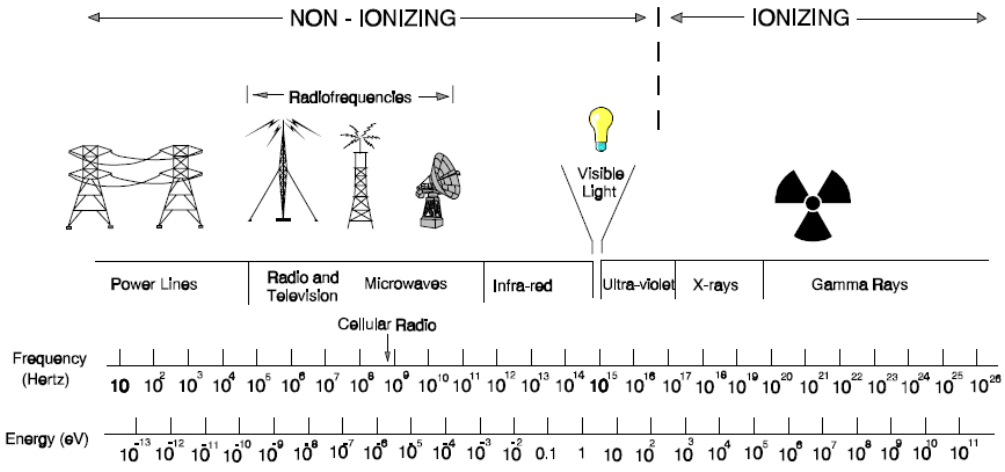

Figure 1.1: The Electromagnetic Spectrum [9]

Temperature elevation is one of the most important factors to induce adverse health effects [8].

Biological effects that result from heating of tissue by RF energy are termed as "thermal" effects [9].

Some biological effects of electromagnetic exposure were noted. Mobile phone radiation can damage DNA. The degree of damage depended on the duration of the exposures. Also recent studies have shown significant reductions in sperm motility, viability and quantity in men using mobile phones for more than a few hours a day [10]. Epidemiologic evidence indicates that mobile phone use of less than 10 years does not pose any increased risk of brain tumour or acoustic neuroma. For long-term use, data are sparse, and the following conclusions are therefore uncertain and controversial. For diseases other than cancer, very little epidemiologic data are avaliable. A particular consideration is mobile phone use by children. While no specific evidence exists, children or adolescents may be more sensitive to RF field exposure than adults. Children of today will also experience a much higher cumulative exposure than previous generations. To date no epidemiologic studies on children available [11].

There are a lot of news, articles, reports, studies on microwave radiation hazard and they report miscellaneous biological effects. Uner and Kramarenko studied the effects of the EMFs emitted by cellular phones on the human EEG in adults and children. They have concluded that the EMFs emitted by cell phones may be harmful for the human brain, since the delta waves are pathological if seen in awake subjects. On the other hand, the slow wave activity was more pronounced in children than adults, probably because absorption of microwaves is greatest in an object about the size of a child's head; the radiation can penetrate the thinner skull of an infant with greater ease [12]. Being exposed to the thermal effect could cause fatigue, cataracts and reduced mental concentration. Research is going on to study the non-thermal effects of radiation, and it has been associated with affecting the cell membrane permeability. Sadly the current exposure safety standards are purely based on the thermal effect while ignoring the non-thermal effects of radiation [13].

Since mobile phones broadcast specifically at frequencies at which the head acts as an antenna and brain tissue acts as a demodulating radio receiver then it is reasonable to expect effects, adverse and otherwise, from bio-resonance at field strengths and specific absorption rates well below current thresholds [14]. In another study, the results showed that radiation from a standard cellular telephone affected the brain electrical activity of rabbits exposed to the radiation under conditions that simulated normal human use of the telephone. The effect was not seen when the possible contribution of the brain to the SAR was minimized [15].

Also there are studies about human eye RF radiation interaction. It is that reported that eye is one of the most affected organ [13], [16], [17].

To investigate biological effects of electromagnetic radiation, so many studies were carried on biological environments and with various biological models at different frequencies. Fujino, Hirata and Shiozawa evaluated the induced SAR in an inhomogenous model of human body for exposure to EM waves from a dipole antenna at 400 MHz. In particular, they compared the results for the homogenous and inhomogenous models and they observed a large difference in the SAR distributions.

Additionally, the peak SARs averaged over 1 g or 10 g of tissue obtained in the homogenous model are overestimated as compared with those in the inhomogenous model, only when the antenna-model distance is small [18]. In another study, the effects of hand-held cellular phones to isolated human head is studied with FDTD method. The comparisons of GSM and DECT systems show the relation between antenna and absorbed powers in human tissues. Tissues are lossy dielectrics and their conductivity values increase with frequency. As the operating frequency increases, the peak SAR value increases but total absorbed power in human head decreases, because of the decrease in penetration of EM fields through tissues.

Optimisation between the peak SAR and total absorbed power should be made in choosing the operating frequency and antenna power for mobile communication systems. Accuracy of numerical simulations strongly depend on the reliability of electrical parameters of the tissues [19].

Lin reports that the uses of anatomically correct models derived from MRI data of children may not be the cause of the difference in the conclusions reached. Additionally, the exploration of a wider range of antenna distances used in the computation both for models of children and for adults may disperse much of the contention [20].

CHAPTER 2

METHOD

Throughout the procedure, a multipole expansion of the fields both in free space and inside the dielectric is used. The multipole coefficients of the scattered field are found by state-space technique. In finding the total field in the dielectric integral expressions for the incident fields are used, the numerically (loop) evaluated incident fields are added to the scattered fields.

Several assumptions have to be made to obtain a solution to this complex problem. First of all it is a difficult task to find out the electrical parameters for each phantom at any frequency. Also the solution would be quite difficult in case the exact shape of the head is to be considered. So the model of the head is assumed to be composed of concentric spheres representing the brain, bone and the skin layers. Each layer have different permittivity and conductivity. Loop antenna excitation is taken in our study. The results taken are for 900 MHz and 1800 MHz GSM frequencies.

2.1 The Theory of State-Space Formulation of Scattering

The general block-diagram of a scattering problem can be illustrated as shown in Fig. 2.1 [21].

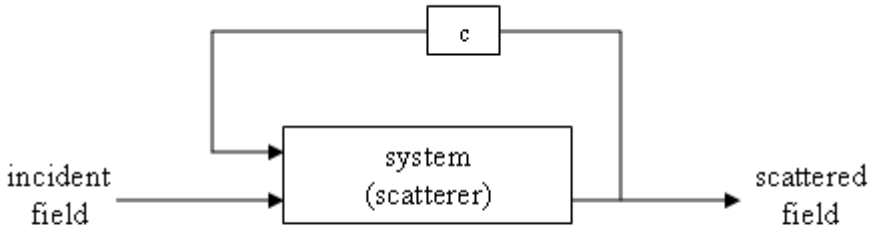

Figure 2.1: Block diagram of scattering

In this case the scatterer is an inhomogenous and lossy dielectric spherical shell which is used as the idealized model for the outer layers (except the brain) of the head and the brain being the homogenous spherical core. Since thin-wire antennas are used, the re-radiation from the antenna is neglected.

2.1.1 The formulation of scattering from inhomogeneous dielectric spherical shells

It is used the formulation provided in [21,22]. Here it is summarized the relevant parts given in [21,22]. The thermal effect of electromagnetic field on bio-objects is directly related to the incident field strength [23]. The incident electromagnetic field induces a volume distribution of the electric polarization current density and the electric conduction current density in the shell of dielectric. These induced sources re-radiate into a source-free region which result in the scattered field. The total field in the air gap is obtained by adding the scattered and the incident fields. Using the boundary conditions on the spherical surface between the dielectric and the gap, the total field in the dielectric is obtained.

2.2 Extension of the Theory to Structures with Homogenous Dielectric Core

2.2.1 General description of the problem

In the model of the head [4], the brain is approximated by a homogenous core covered by inhomogenous core covered by inhomogenous dielectric layers, representing the brain, bone and skin layers. All the layers including the brain are lossy, isotropic and dispersive. This model will be excited by loop antenna placed outside the structure. The distribution of the heating potential P_p $(in\, Watt/m^3)$ inside the dielectric structure is then evaluated with the exciting source being either a thin-wire loop antenna with constant current with piecewice-continuous sinusoidal current distribution. The heating potential is then

$$P_p(R,\theta,\phi) = \sigma(R)\left|\bar{E}(R,\theta,\phi)\right|^2 / 2 \tag{2.1}$$

where $\sigma(R)$ is the conductivity and $\bar{E}(R,\theta,\phi)$ is the electric field inside the head.

The loop is assumed to be infinitesimally thin and electrically small, i.e $2\pi a_1 < \lambda$, a_1 being the loop radius and λ is the wavelength.

Under these conditions a constant current (I_0) flowing through the loop can be realizable.

A loop antenna that is located R_{12} distance from origin generates E-field as

$$\bar{E} = \frac{j\mu a_1 I_0 f}{2}\int_0^{2\pi} \cos\phi_s \frac{e^{jkR_s}}{R_s} d\phi_s \hat{u}_\phi \tag{2.2}$$

where $R_s = \left[(R_s\cos\theta_s - R_{12})^2 + (R_s\sin\theta_s - a_1\cos\phi_s)^2 + a_1{}^2\sin^2\phi_s\right]^{1/2}$ (2.3)

the antenna is made of thin wire, f is the frequency, I_0 is constant current that flows in the antenna, μ is permeability, ϕ_s is azimuth angle on the antenna, $\hat{u}_\phi$ is unit vector in azimuth angle direction.

The head configuration that is used in this study is shown in Figure 2.2. The head model is three concentric spheres that are composed of the brain having 9 cm radius, the bone having 5 mm thickness and the skin having 5 mm thickness. This head model is excited by a loop antenna that has a_1 radius and located R_{12} distance from origin at 900 MHz and 1800 MHz. The complex dielectric parameters of the head model is as seen in Table 2.1 [1]. In Figure 2.2, θ expresses zenith angle, R expresses radial coordinate in θ direction. In Table 2.1, ε_r expresses permittivity, σ expresses conductivity. Coordinates of head and coordinates of antenna are different from each other, (R_s, θ_s, ϕ_s) expresses coordinates of antenna.

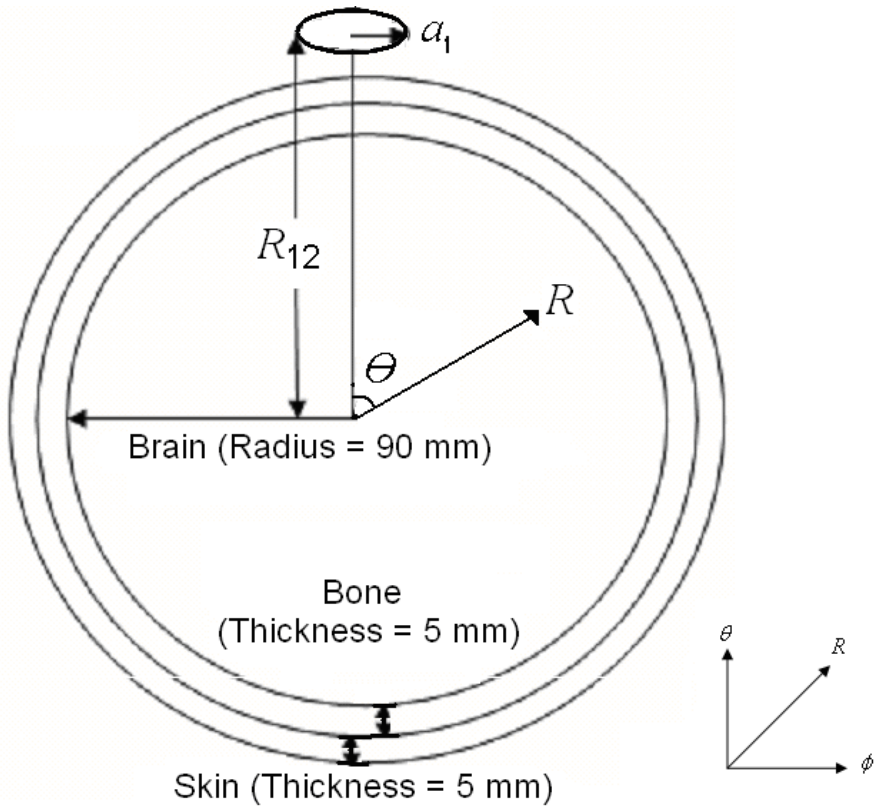

Figure 2.2: Spherical head model and configuration

Table 2.1: Complex dielectric specifications of the head model that is used in simulation [1]

Layer	**Radius (mm)**	**900 MHz** ε_r	**900 MHz** σ **(mmho/m)**	**1800 MHz** ε_r	**1800 MHz** σ	**Mass Density** $\left(kg/m^3\right)$
Skin	100	39,5	700	38,2	900	1080
Bone (cortical)	95	12,5	170	12,0	290	1180
Brain (Grey matter)	90	56,8	1100	51,8	1500	1050

Scattered field is found using multipole expansion coefficients, multipole expansion coefficients are solved using state-space equations by computer program that are developed by using Fortran programming language.

With the aid of total E-field heating potential in the dielectric structure is found [21].

CHAPTER 3

THE DISTRIBUTION OF THE HEATING POTENTIAL IN THE HEAD MODEL

Using equation 2.2 heating distributions in head were plotted. The plots that are between Figure 3.1 and Figure 3.4 show the heat profiles for f = 900 MHz, R_{12} = 10 cm, 12 cm, 14 cm, 16 cm, respectively. The plots that are between Figure 3.5 and Figure 3.8 show heat profiles at the same parameters for f = 1800 MHz, R_{12} = 10 cm, 12 cm, 14 cm, 16 cm, respectively. All these plots between Figure 3.1 and Figure 3.8 are for $ka_1 = 0{,}3$. $I_0 = 1\ \mu A$ is taken in all these figures.

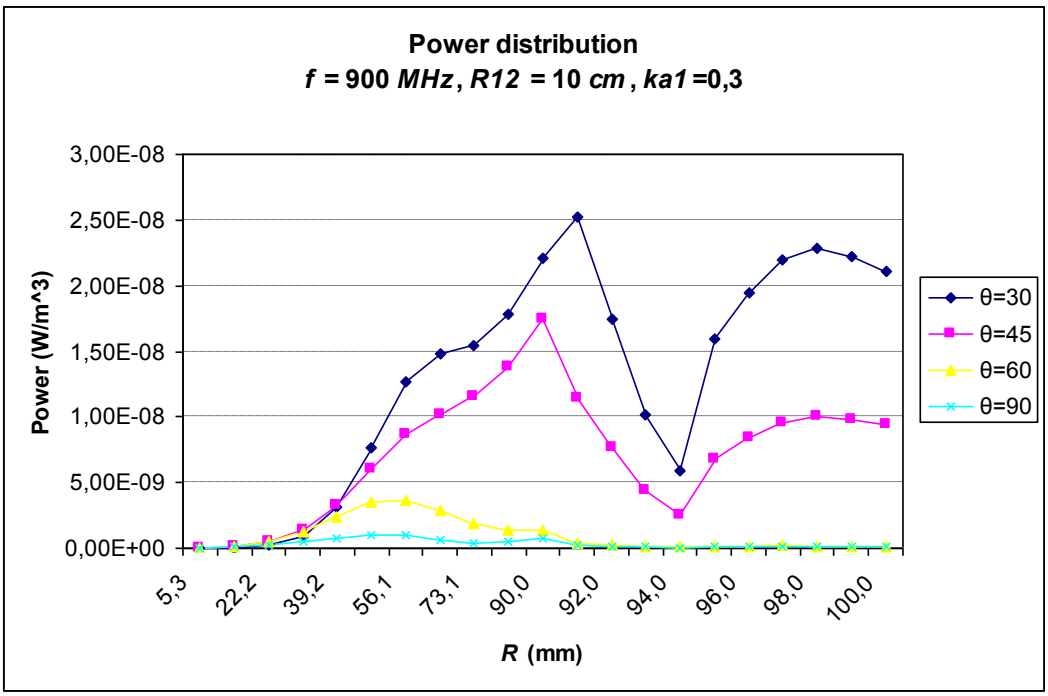

Figure 3.1: Heating potential at f = 900 *MHz*, R_{12}=10 *cm*, ka_1=0,3

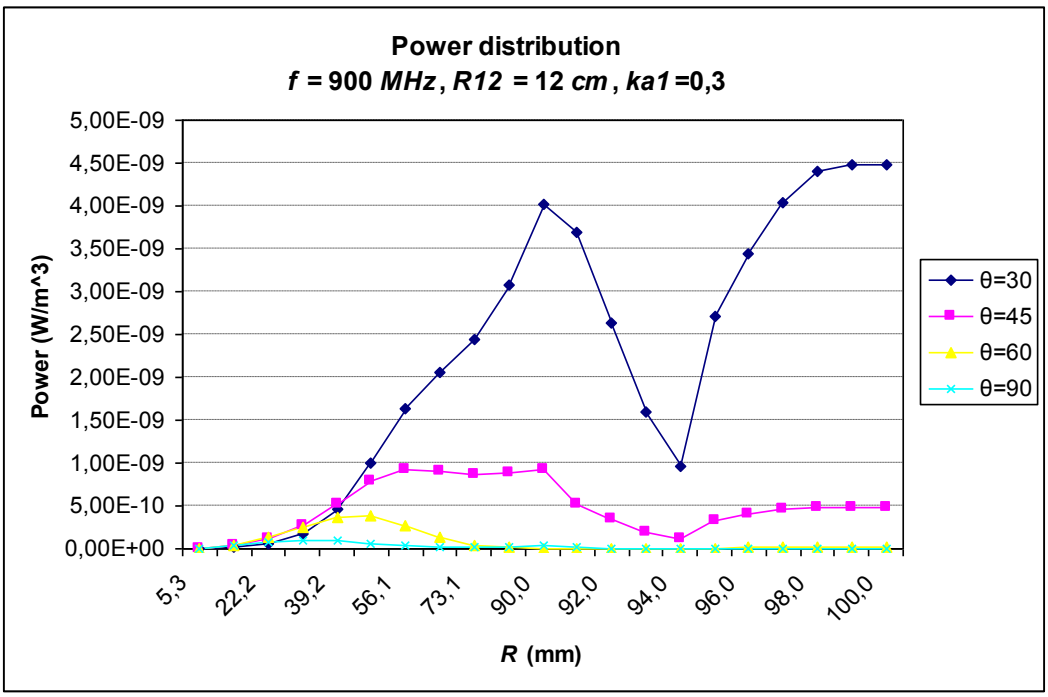

Figure 3.2: Heating potential at f = 900 *MHz*, R_{12}=12 *cm*, ka_1=0,3

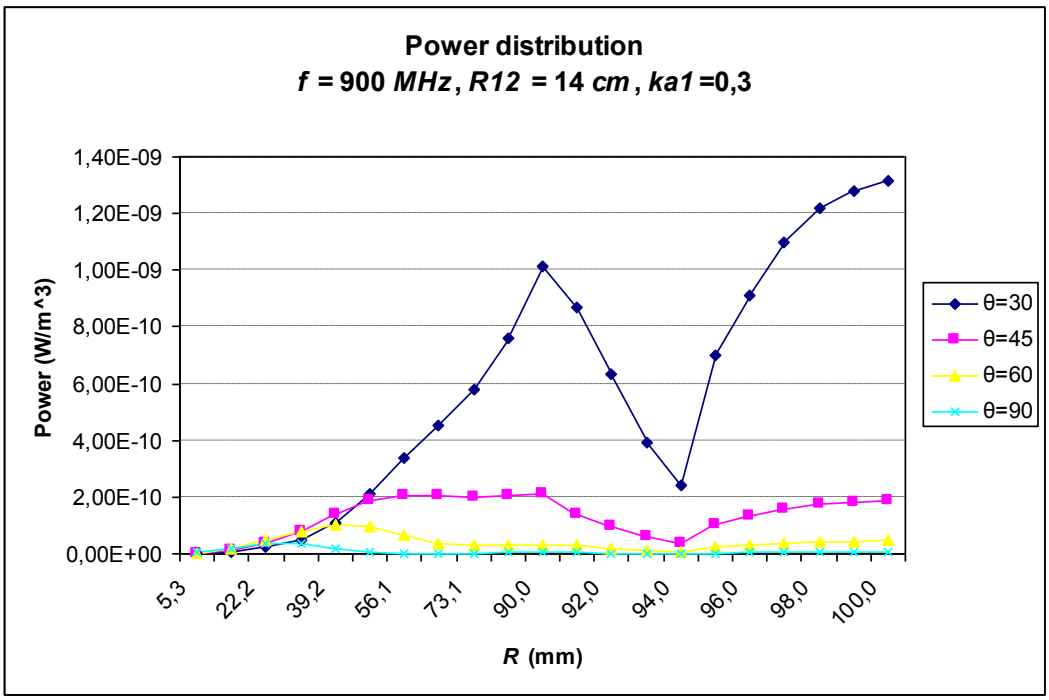

Figure 3.3: Heating potential at f = 900 *MHz*, R_{12}=14 *cm*, ka_1=0,3

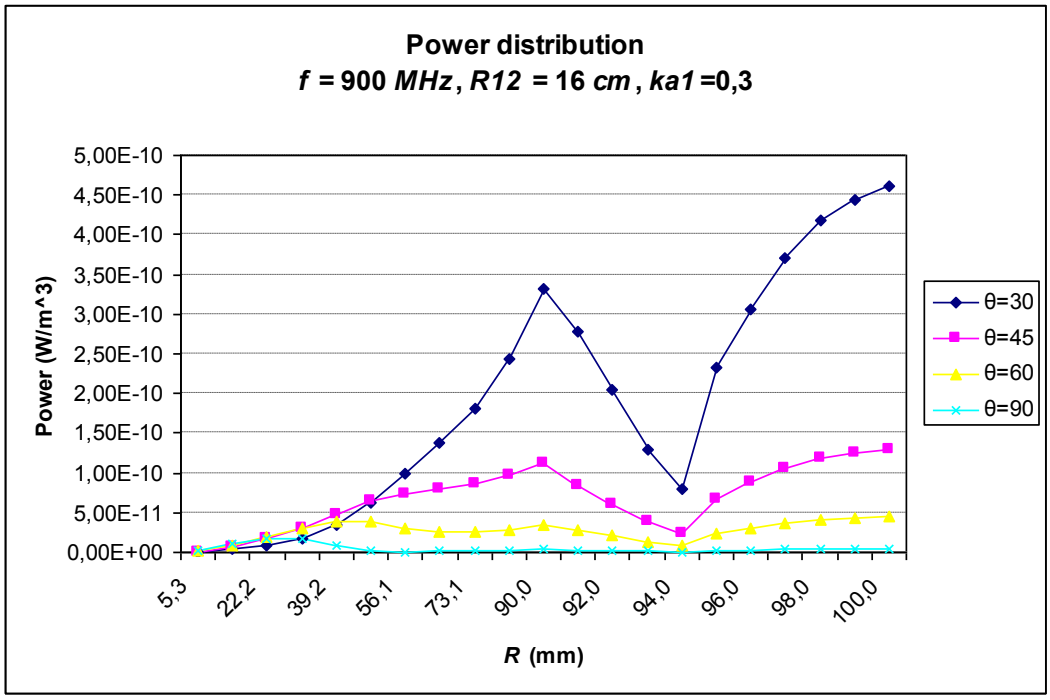

Figure 3.4: Heating potential at f = 900 *MHz*, R_{12}=16 *cm*, ka_1=0,3

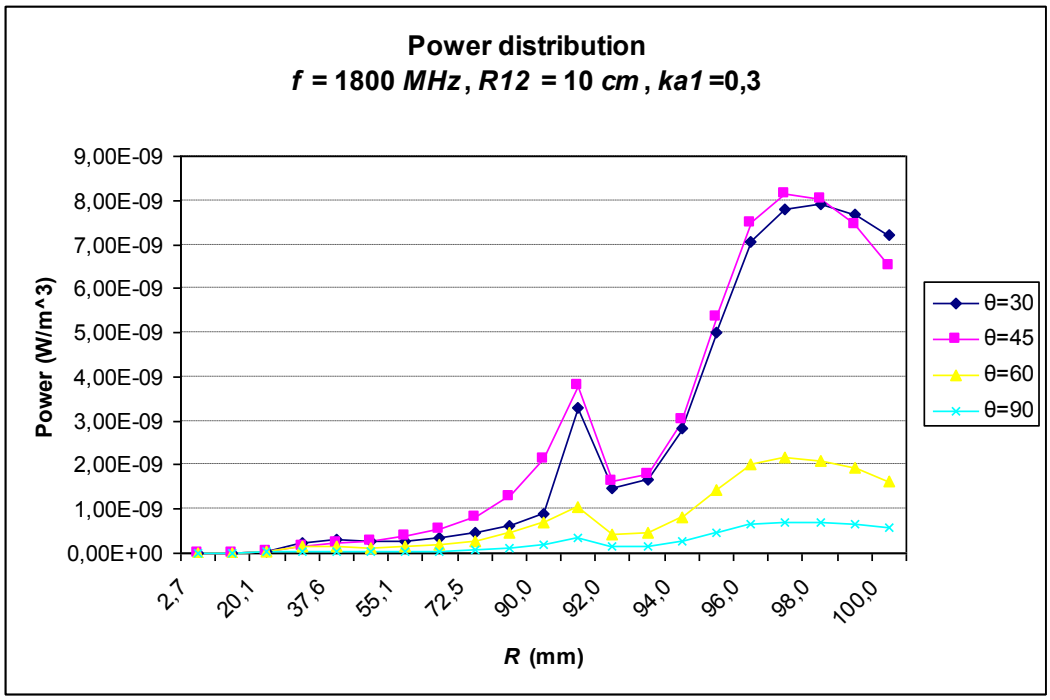

Figure 3.5: Heating potential at f = 1800 *MHz*, R_{12}=10 *cm*, ka_1=0,3

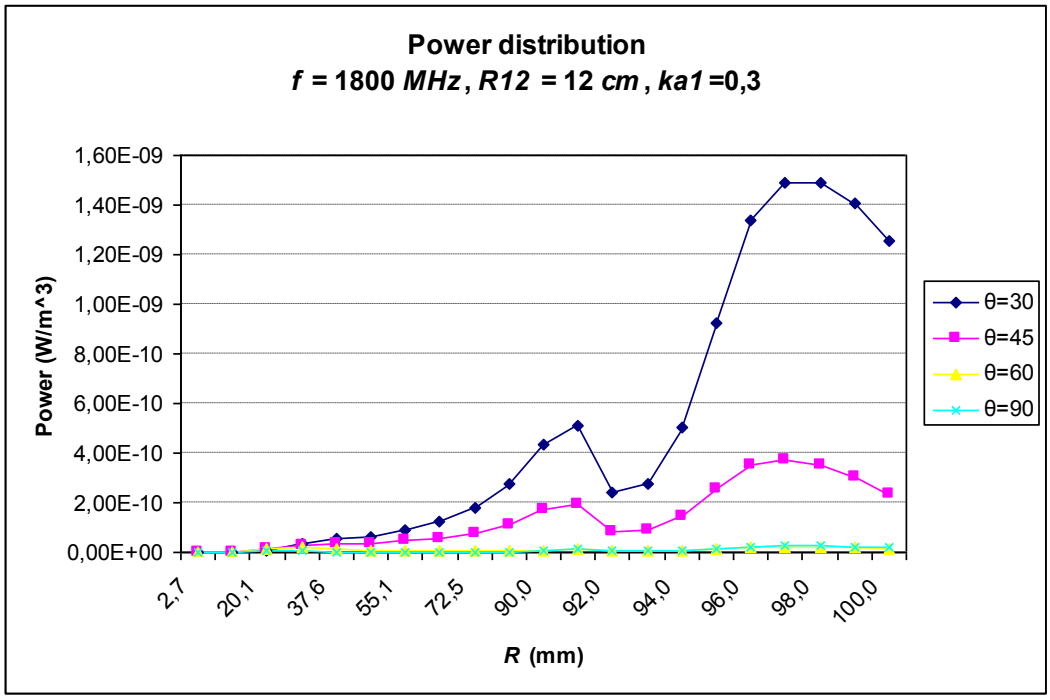

Figure 3.6: Heating potential at f = 1800 *MHz*, R_{12}=12 *cm*, ka_1=0,3

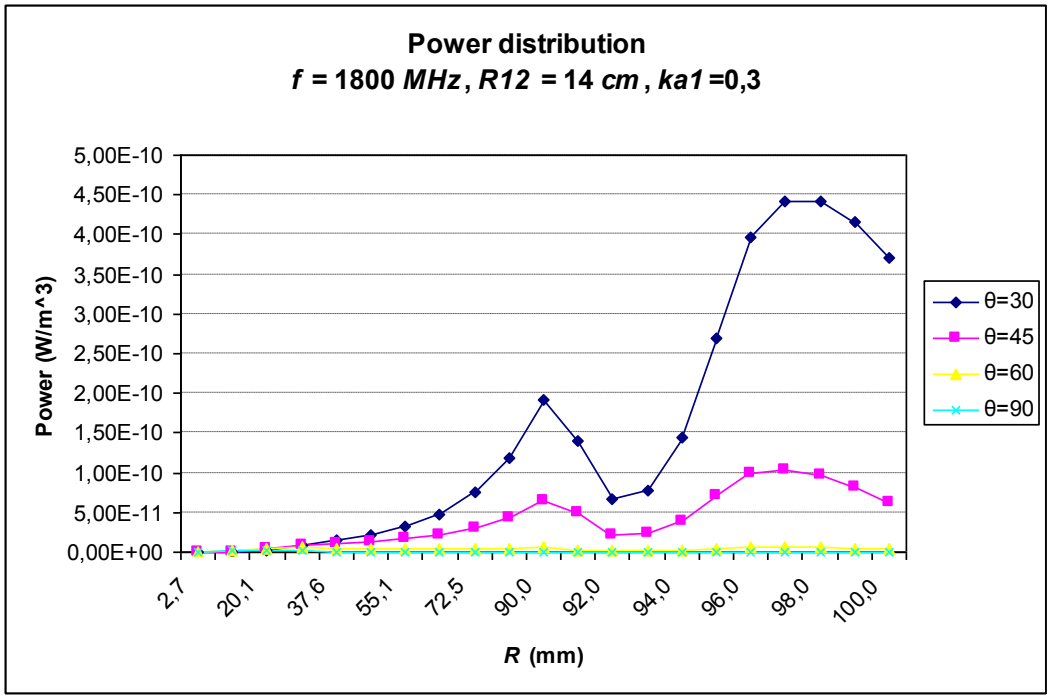

Figure 3.7: Heating potential at f = 1800 *MHz*, R_{12}=14 *cm*, ka_1=0,3

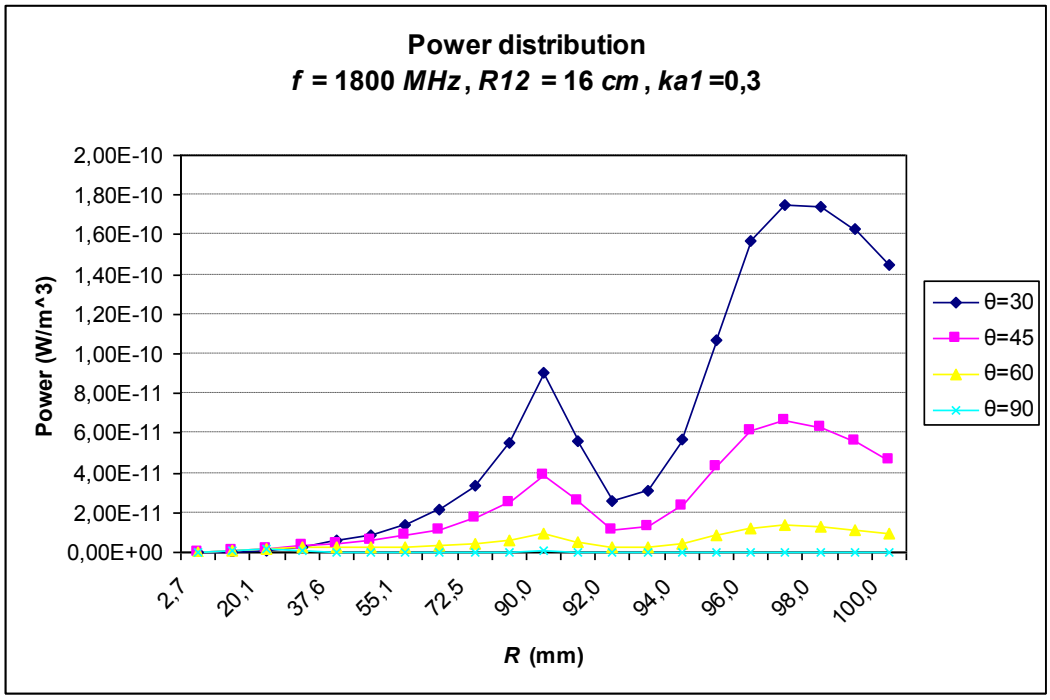

Figure 3.8: Heating potential at f = 1800 *MHz*, R_{12}=16 *cm*, ka_1=0,3

As shown in Figure 3.1, the heat increases as we go from the center of the head to outer layer, decreases at the bone layer because of the low conductivity and again increases at the skin layer at 900 MHz, for $\theta = 30^0$. In all the dielectric structures, maximum heat is found at the skin and the area that join the brain and the bone. Two point that should be underlined are the radiation distance and conductivity value. For bigger θ, heat value decreases on radial axis and maximum heat is obtained about the center of the head. As seen in Figure 3.2, Figure 3.3 and Figure 3.4, heat values decrease while R_{12} distance increases. The comments for 900 MHz are substantially acceptable for 1800 MHz but absolute heat values are less than the values for 900 MHz.

Electromagnetic radiation definitions and standardizations are available in Table 3.1 [9].

Table 3.1: FCC Limits for Localized (Partial-body) Exposure

Specific Absorption Rate (SAR)	
Occupational/Controlled Exposure (100 kHz – 6 GHz)	General/Uncontrolled Exposure (100 kHz - 6 GHz)
< 0,4 W/kg whole-body ≤ 8 W/kg partial-body	< 0,08 W/kg whole-body ≤ 1,6 W/kg partial-body

For 900 MHz and 1800 MHz, SAR (Specific Absorption Rate) values were calculated by dividing maximum power value into mass density for maximum power absorption situation. According to these criterion, for $I_0 = 1\,\mu A$ obtained SAR values are all lower than the specified limits.

Table 3.2: For R_{12}=10 *cm* absorbed max. power, SAR values

	900 MHz			**1800 MHz**		
θ	**Mass Density (kg/m^3)**	**Max. Power (W/m^3)**	**SAR (W/kg)**	**Mass Density (kg/m^3)**	**Max. Power (W/m^3)**	**SAR (W/kg)**
30^0	1180	2,52E-08	2,13E-11	1180	7,90E-09	6,69E-12
45^0	1050	1,74E-08	1,66E-11	1180	8,15E-09	6,91E-12
60^0	1050	3,66E-09	3,48E-12	1180	2,17E-09	1,84E-12
90^0	1050	1,02E-09	9,74E-13	1180	7,15E-10	6,06E-13

Table 3.3: For R_{12}=12 *cm* absorbed max. power, SAR values

	900 MHz			**1800 MHz**		
θ	**Mass Density (kg/m^3)**	**Max. Power (W/m^3)**	**SAR (W/kg)**	**Mass Density (kg/m^3)**	**Max. Power (W/m^3)**	**SAR (W/kg)**
30^0	1080	4,48E-09	4,15E-12	1080	1,49E-09	1,38E-12
45^0	1080	4,90E-10	4,53E-13	1080	3,72E-10	3,44E-13
60^0	1050	3,92E-10	3,73E-13	1080	2,09E-11	1,94E-14
90^0	1050	8,75E-11	8,33E-14	1080	2,51E-11	2,33E-14

Table 3.4: For R_{12}=14 *cm* absorbed max. power, SAR values

	900 MHz			1800 MHz		
θ	Mass Density (kg/m^3)	Max. Power (W/m^3)	SAR (W/kg)	Mass Density (kg/m^3)	Max. Power (W/m^3)	SAR (W/kg)
30^0	1080	1,32E-09	1,22E-12	1080	4,43E-10	4,10E-13
45^0	1050	2,11E-10	2,01E-13	1080	1,05E-10	9,68E-14
60^0	1050	1,00E-10	9,53E-14	1050	6,31E-12	6,01E-15
90^0	1050	3,65E-11	3,47E-14	1050	2,73E-12	2,60E-15

Table 3.5: For R_{12}=16 *cm* absorbed max. power, SAR values

	900 MHz			1800 MHz		
θ	Mass Density (kg/m^3)	Max. Power (W/m^3)	SAR (W/kg)	Mass Density (kg/m^3)	Max. Power (W/m^3)	SAR (W/kg)
30^0	1080	4,62E-10	4,28E-13	1080	1,75E-10	1,62E-13
45^0	1080	1,28E-10	1,19E-13	1080	6,61E-11	6,12E-14
60^0	1080	4,51E-11	4,18E-14	1080	1,34E-11	1,24E-14
90^0	1050	1,76E-11	1,68E-14	1050	1,42E-12	1,35E-15

The plots from Figure 3.9 to Figure 3.12 were obtained for $a_1 = 1cm$ and same head model. Maximum power value was obtained for $\theta = 30^0$ and power value decreases while the distance R_{12} increases.

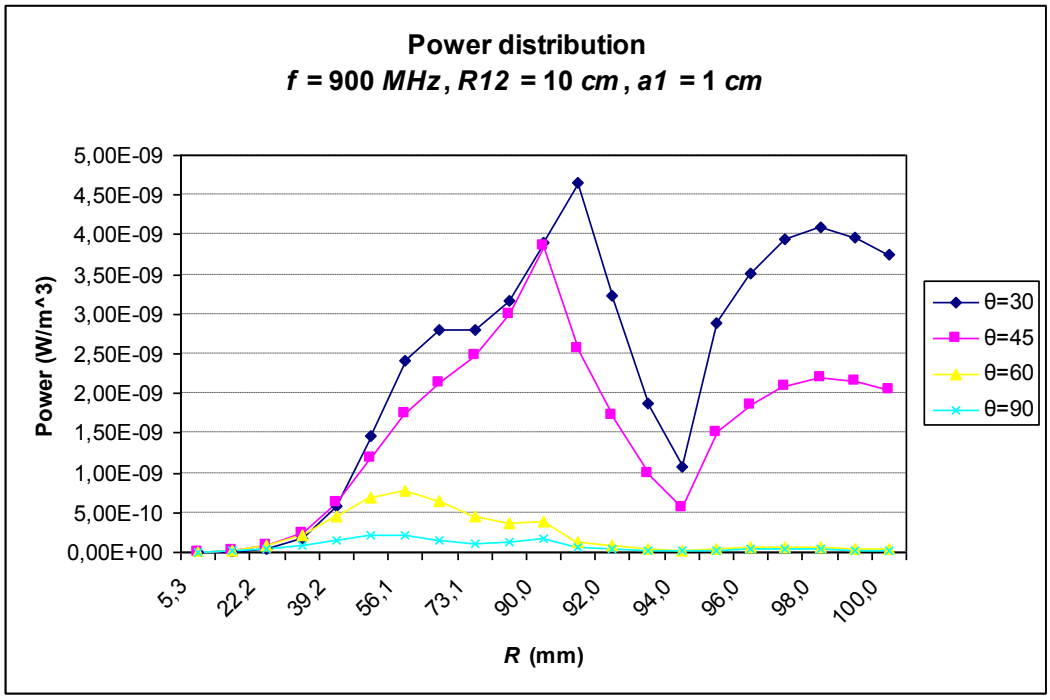

Figure 3.9: Heating potential at f = 900 *MHz*, R_{12}=10 *cm*, a_1=1 *cm*

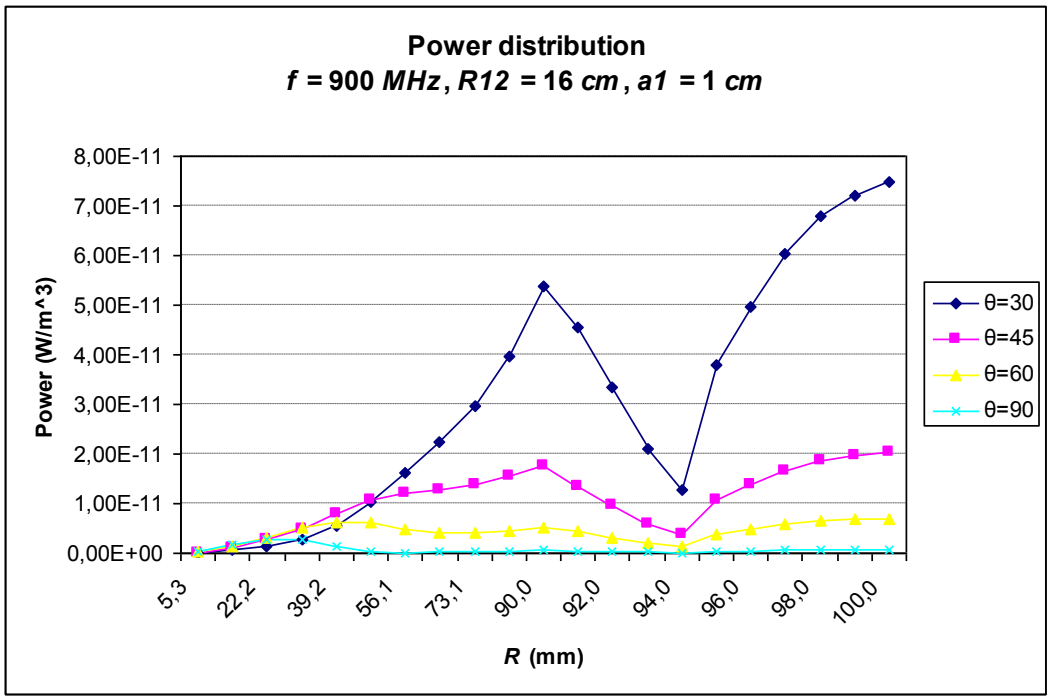

Figure 3.10: Heating potential at f = 900 *MHz*, R_{12}=16 *cm*, a_1=1 *cm*

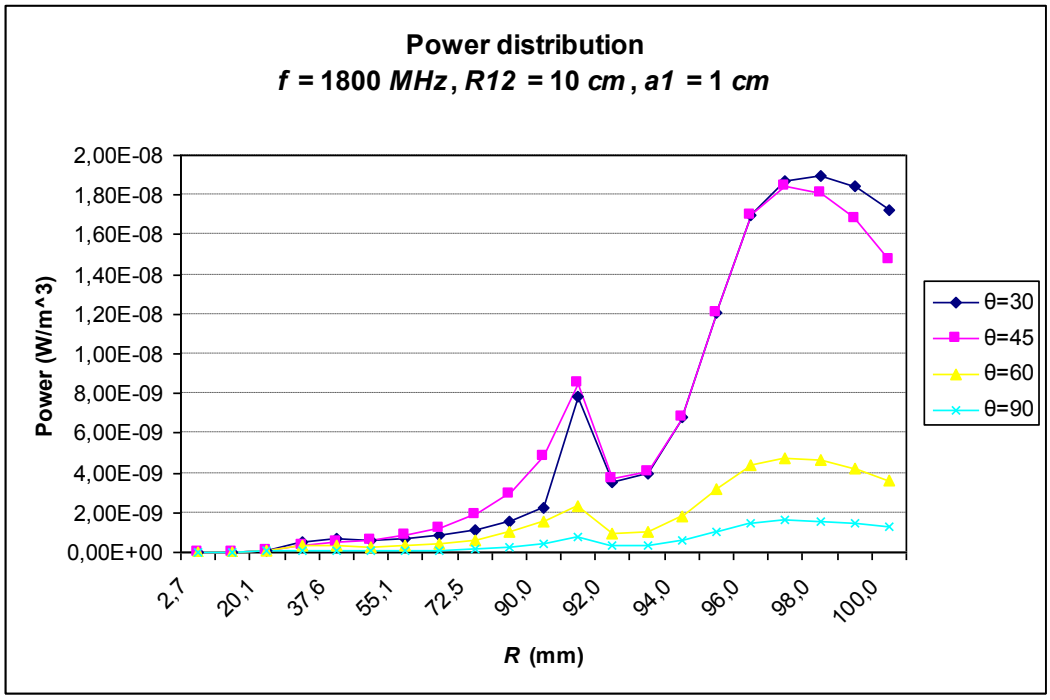

Figure 3.11: Heating potential at f =1800 *MHz*, R_{12}=10 *cm*, a_1=1 *cm*

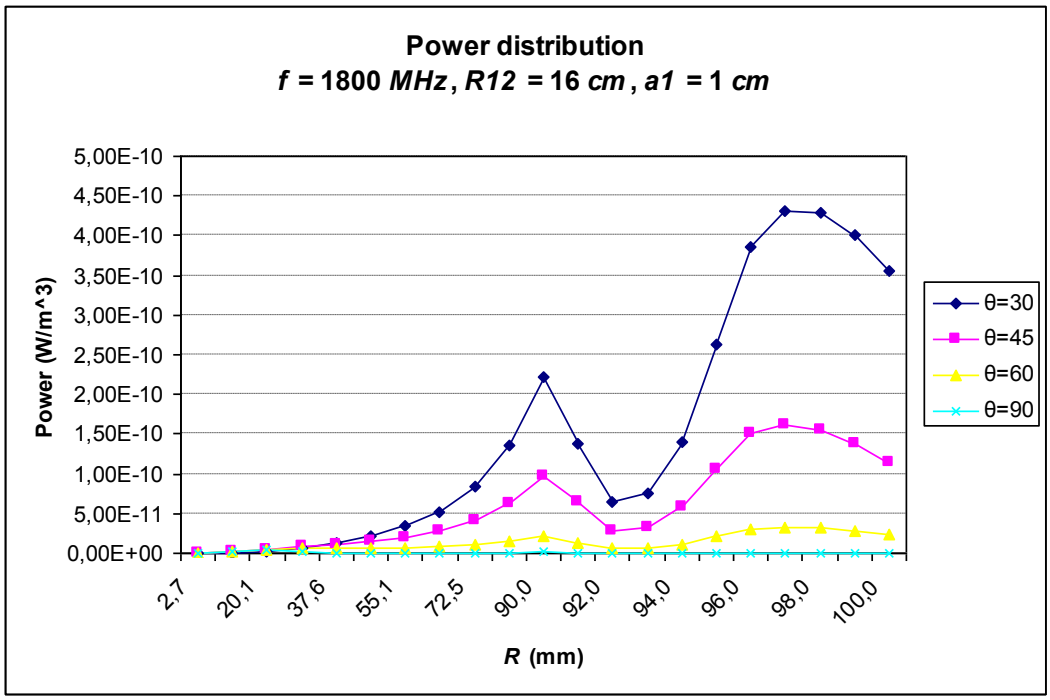

Figure 3.12: Heating potential at f =1800 *MHz*, R_{12}=16 *cm*, a_1=1 *cm*

Table 3.6 and Table 3.7 were obtained for a_1=1 *cm.*

Table 3.6: For R_{12}=10 *cm* absorbed max. power, SAR values

	900 MHz			1800 MHz		
θ	Mass Density (kg/m^3)	Max. Power (W/m^3)	SAR (W/kg)	Mass Density (kg/m^3)	Max. Power (W/m^3)	SAR (W/kg)
30^0	1180	4,66E-09	3,95E-12	1080	1,90E-08	1,76E-11
45^0	1050	3,87E-09	3,68E-12	1080	1,84E-08	1,71E-11
60^0	1050	7,74E-10	7,38E-13	1080	4,78E-09	4,43E-12
90^0	1050	2,16E-10	2,06E-13	1080	1,62E-09	1,50E-12

Table 3.7: For R_{12}=16 *cm* absorbed max. power, SAR values

	900 MHz			1800 MHz		
θ	Mass Density (kg/m^3)	Max. Power (W/m^3)	SAR (W/kg)	Mass Density (kg/m^3)	Max. Power (W/m^3)	SAR (W/kg)
30^0	1080	7,49E-11	6,94E-14	1080	4,30E-10	3,98E-13
45^0	1080	2,02E-11	1,87E-14	1080	1,63E-10	1,51E-13
60^0	1080	7,05E-12	6,53E-15	1080	3,31E-11	3,07E-14
90^0	1050	2,81E-12	2,67E-15	1050	3,49E-12	3,32E-15

CHAPTER 4

RELATION BETWEEN PERMITTIVITY, CONDUCTIVITY AND HEATING POTENTIAL

To investigate the relation between permittivity, conductivity and heating potential, the results were obtained for 10 mm and 20 mm radius spherical objects at different permittivity and conductivity values. This object may be a biological organism/tissue or a substance.

The plots from Figure 4.1 to Figure 4.8 show heating potential of the object with 10 mm radius. Here R1 denotes the radius of the spherical object. Maximum power was obtained surface of the object and at $\theta = 45^0$.

The plots from Figure 4.9 and Figure 4.16 show heating potential of the object with 20 mm radius. Maximum power was obtained surface of the object and $\theta = 30^0$ except f = 1800 *MHz*, $\varepsilon_r = 100, \sigma = 100$ situation. For this situation maximum power was obtained center of the object and $\theta = 45^0$ as seen in Figure 4.14.

Tables 4.1-4.8 show that heating potential at 1800 MHz is higher than at 900 MHz.

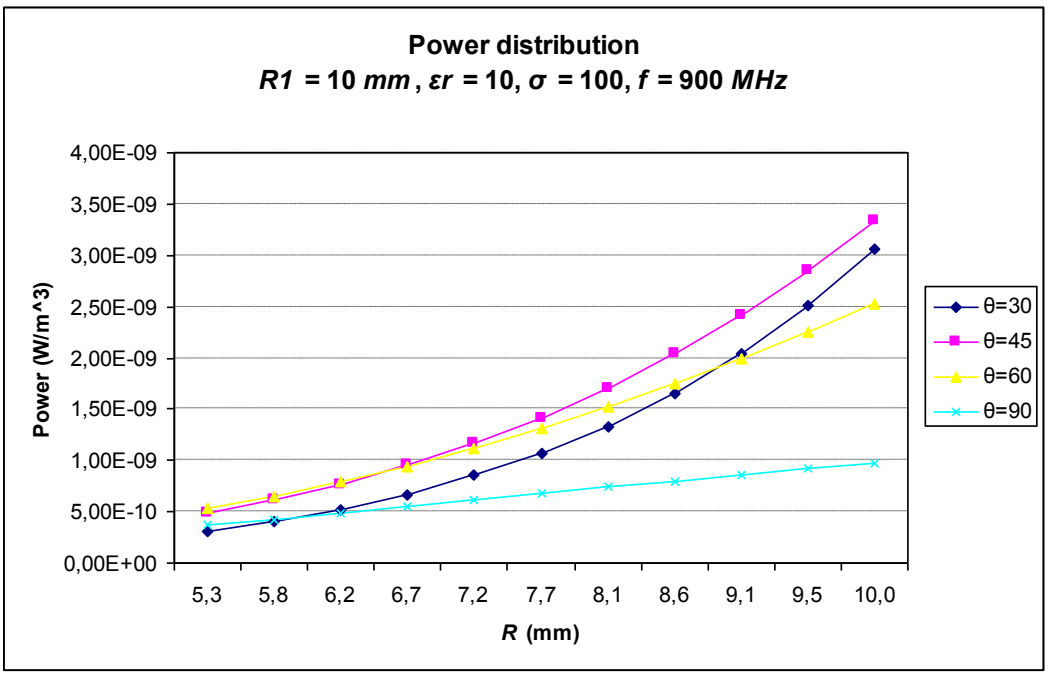

Figure 4.1: Heating potential at f =900 *MHz*, R_{12}=2 *cm*, a_1=1 *cm*

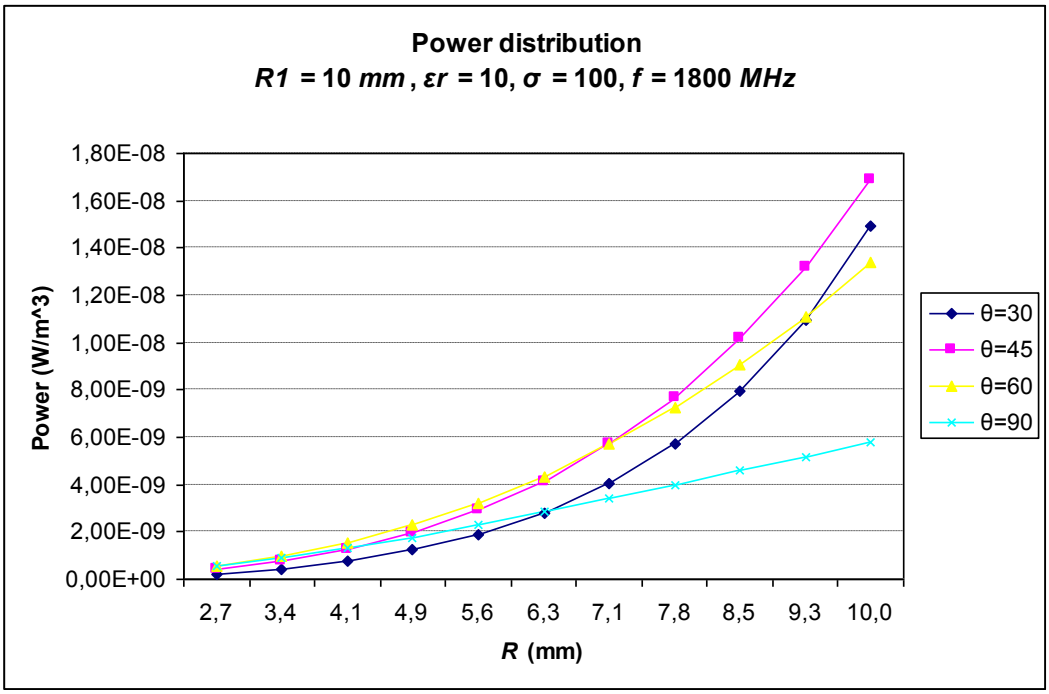

Figure 4.2: Heating potential at f =1800 *MHz*, R_{12}=2 *cm*, a_1=1 *cm*

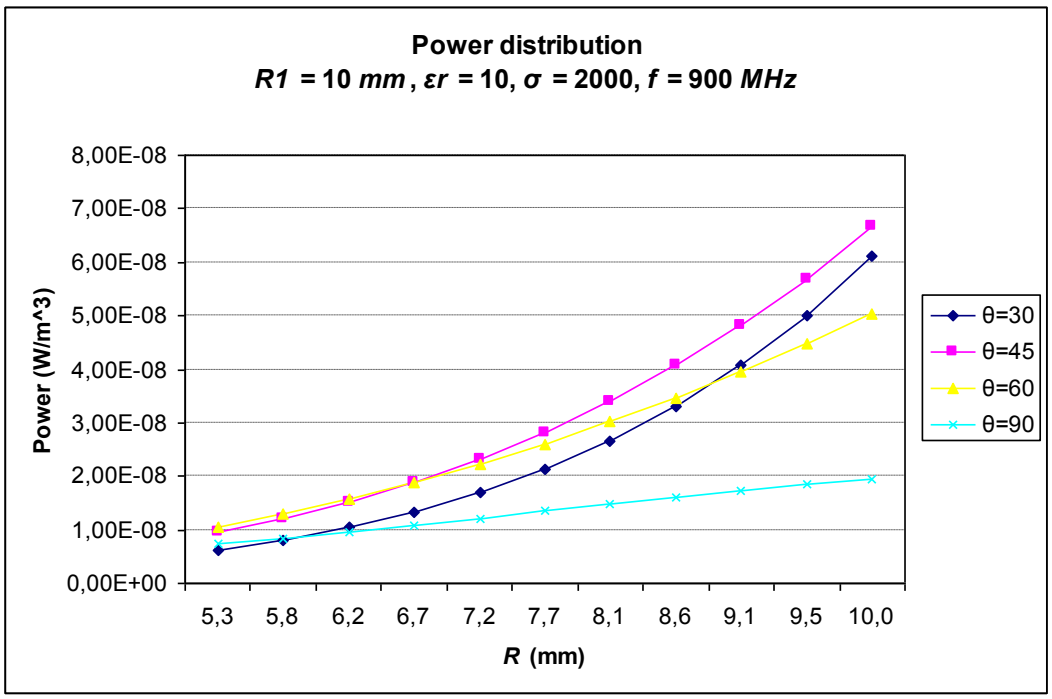

Figure 4.3: Heating potential at f =900 *MHz*, R_{12}=2 *cm*, a_1=1 *cm*

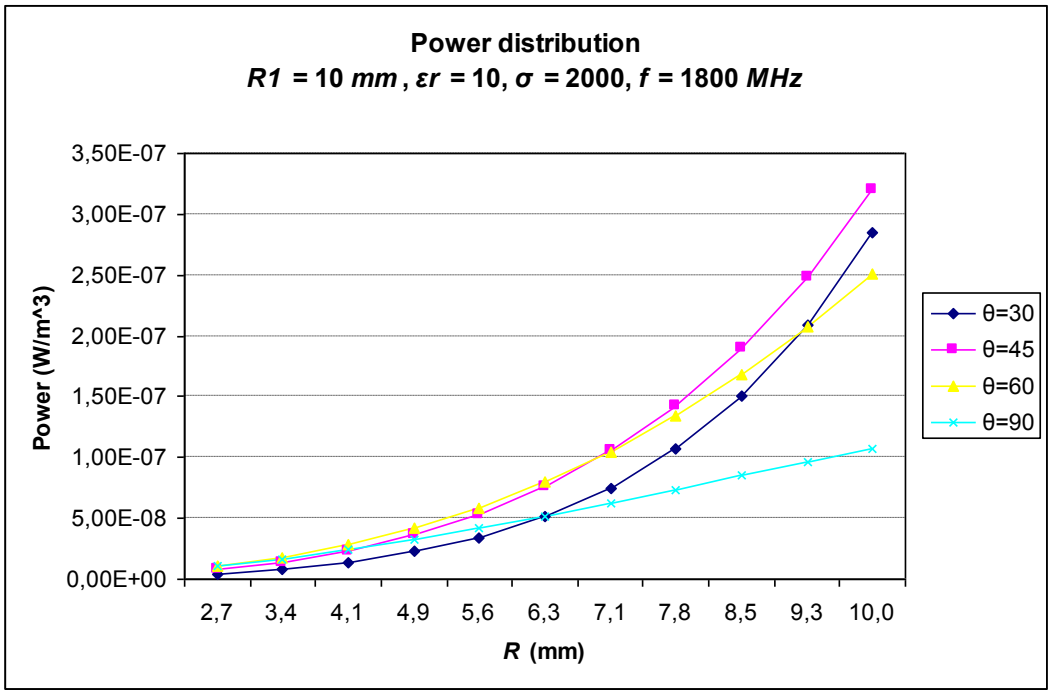

Figure 4.4: Heating potential at f =1800 *MHz*, R_{12}=2 *cm*, a_1=1 *cm*

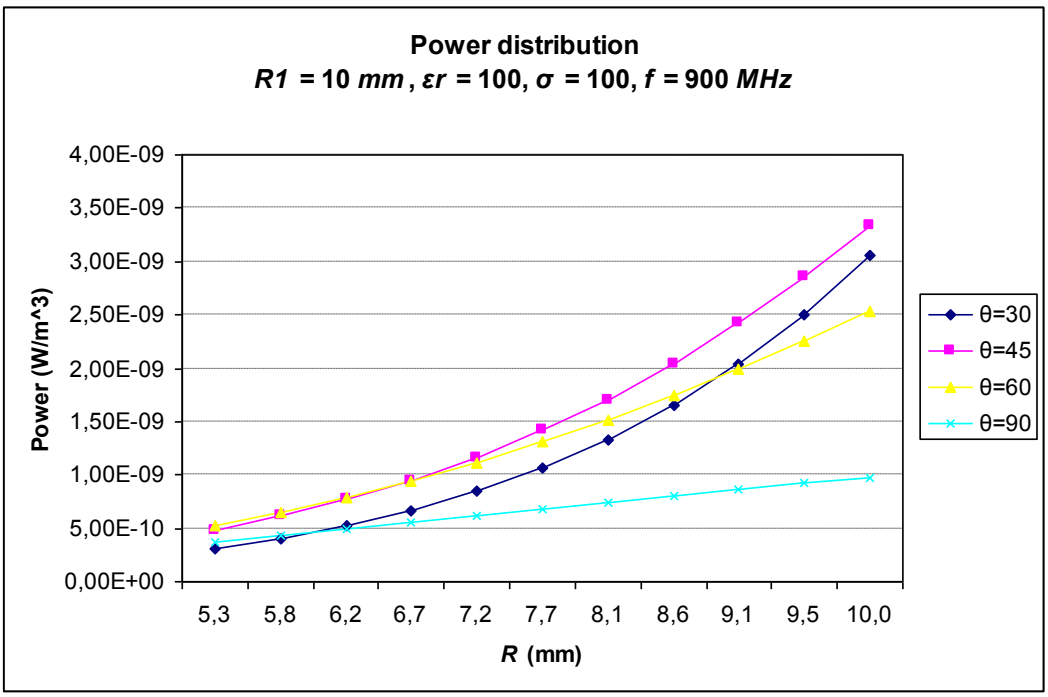

Figure 4.5: Heating potential at f =900 *MHz*, R_{12}=2 *cm*, a_1=1 *cm*

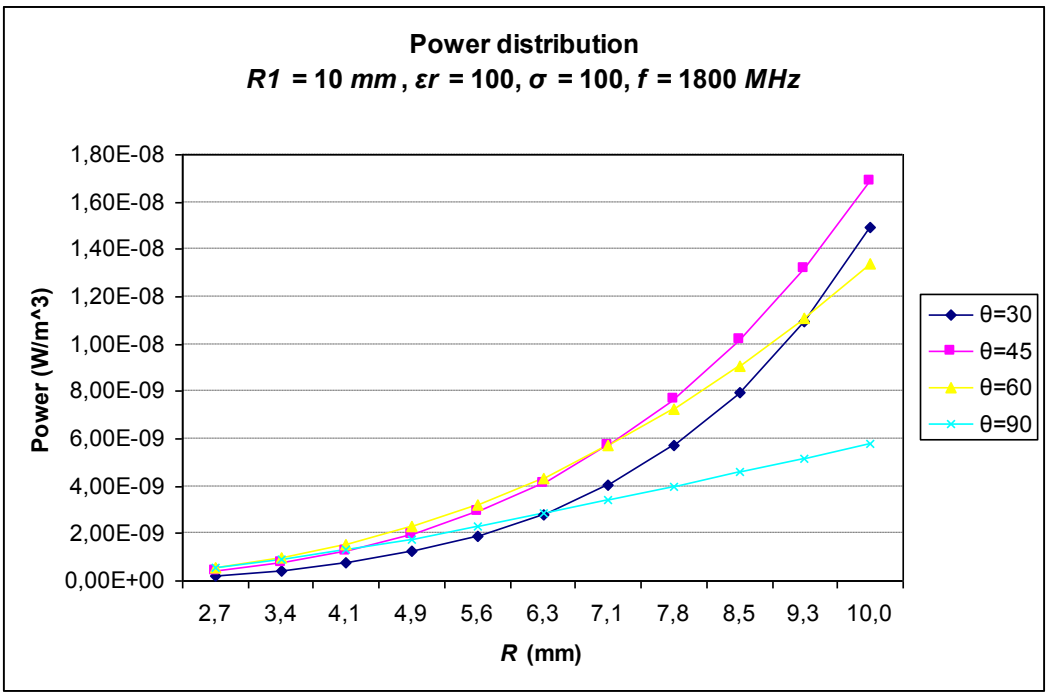

Figure 4.6: Heating potential at f =1800 *MHz*, R_{12}=2 *cm*, a_1=1 *cm*

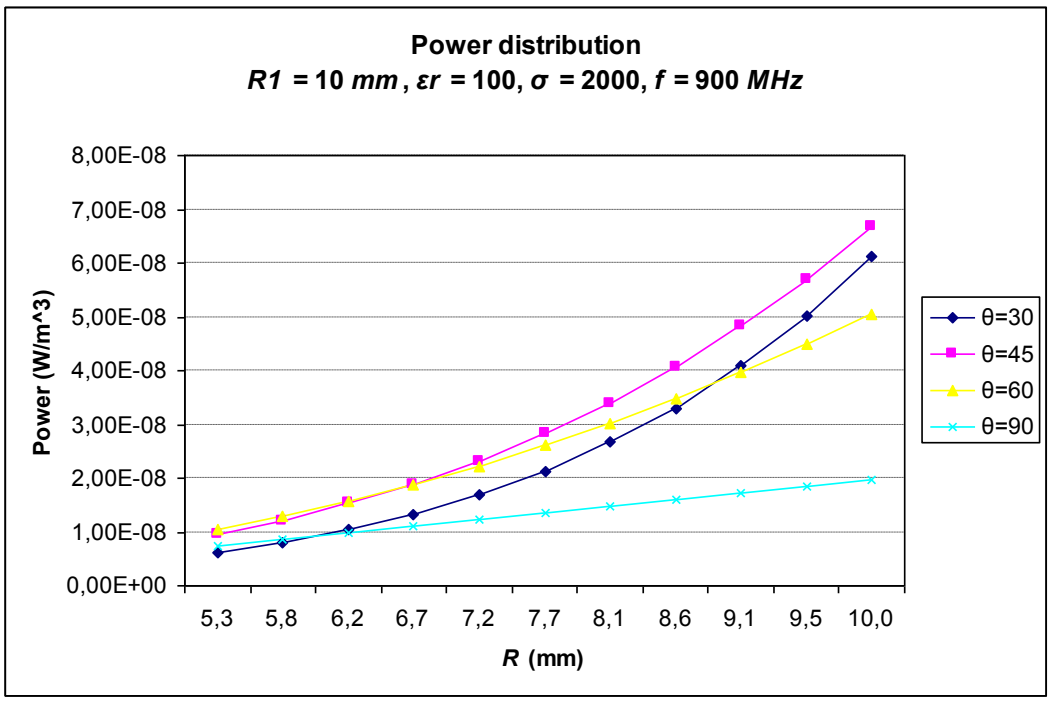

Figure 4.7: Heating potential at f =900 *MHz*, R_{12}=2 *cm*, a_1=1 *cm*

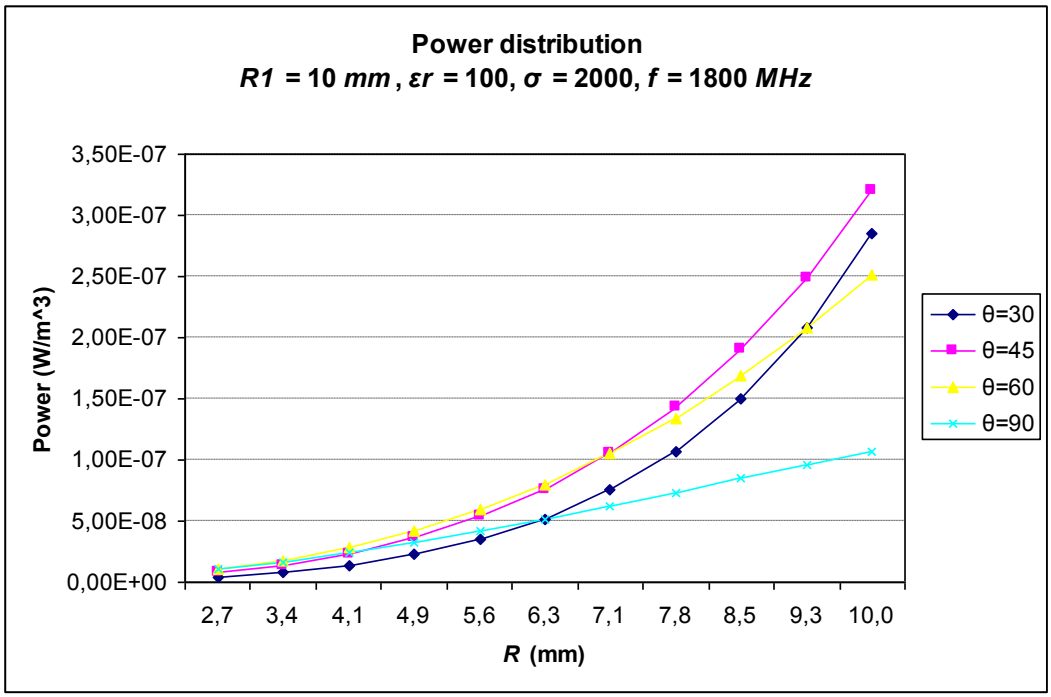

Figure 4.8: Heating potential at f =1800 *MHz*, R_{12}=2 *cm*, a_1=1 *cm*

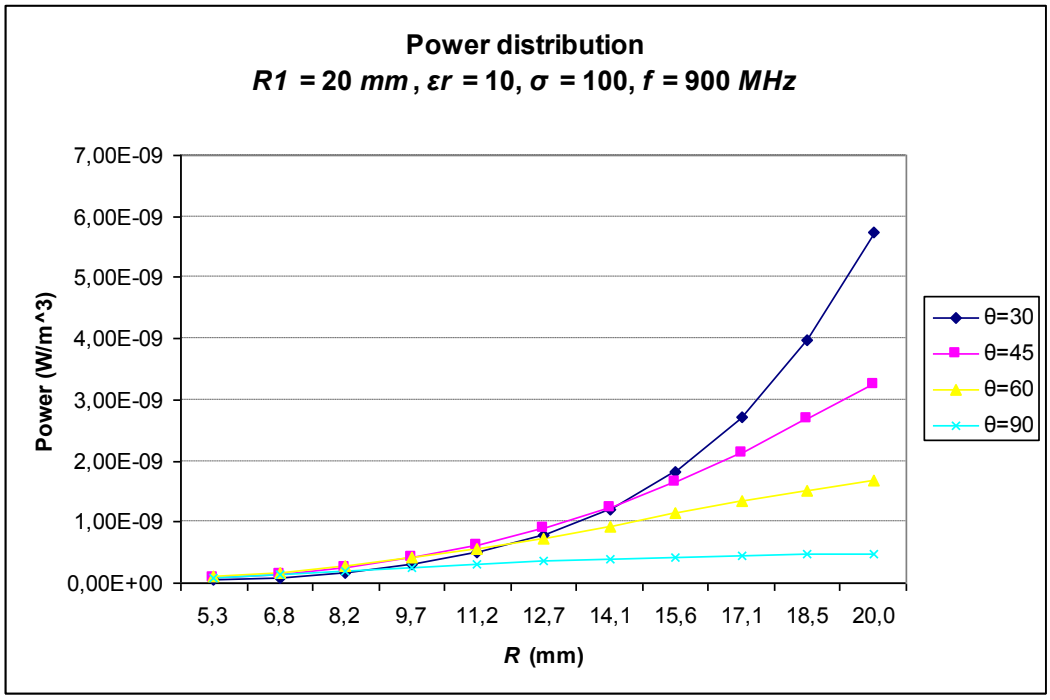

Figure 4.9: Heating potential at f =900 *MHz*, R_{12}=3 *cm*, a_1=1 *cm*

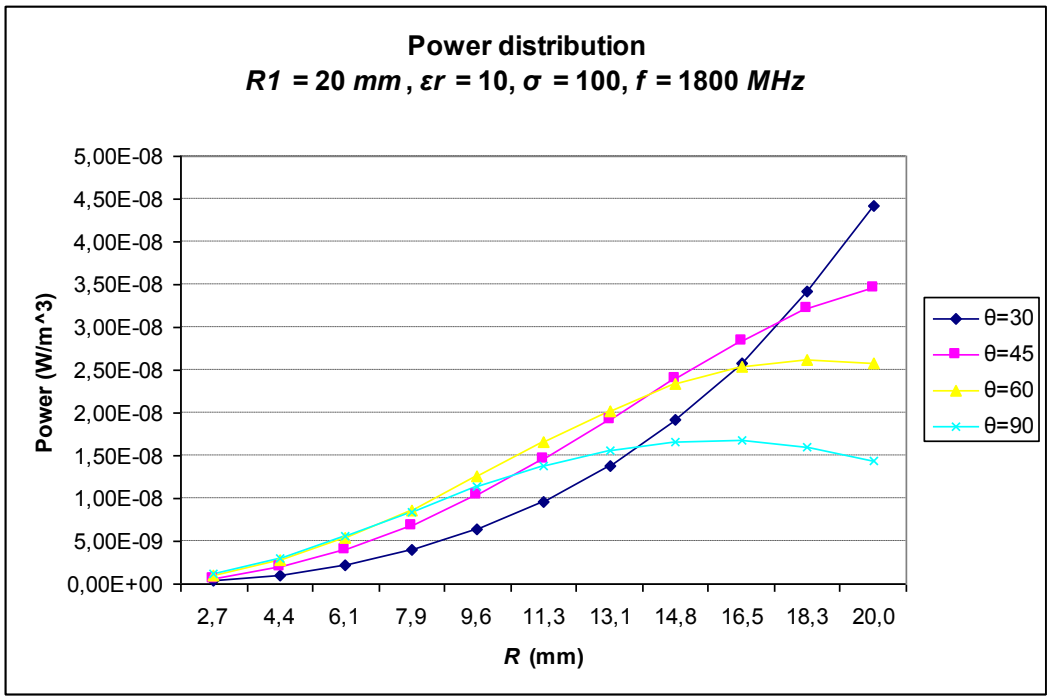

Figure 4.10: Heating potential at f =1800 *MHz*, R_{12}=3 *cm*, a_1=1 *cm*

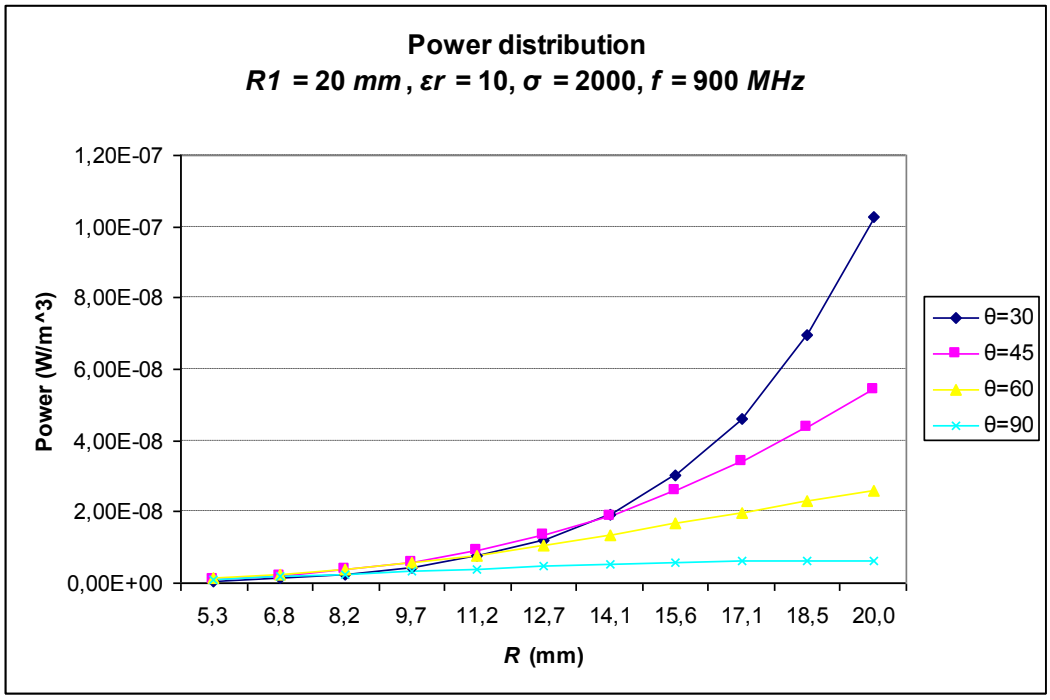

Figure 4.11: Heating potential at *f* =900 *MHz*, R_{12}=3 *cm*, a_1=1 *cm*

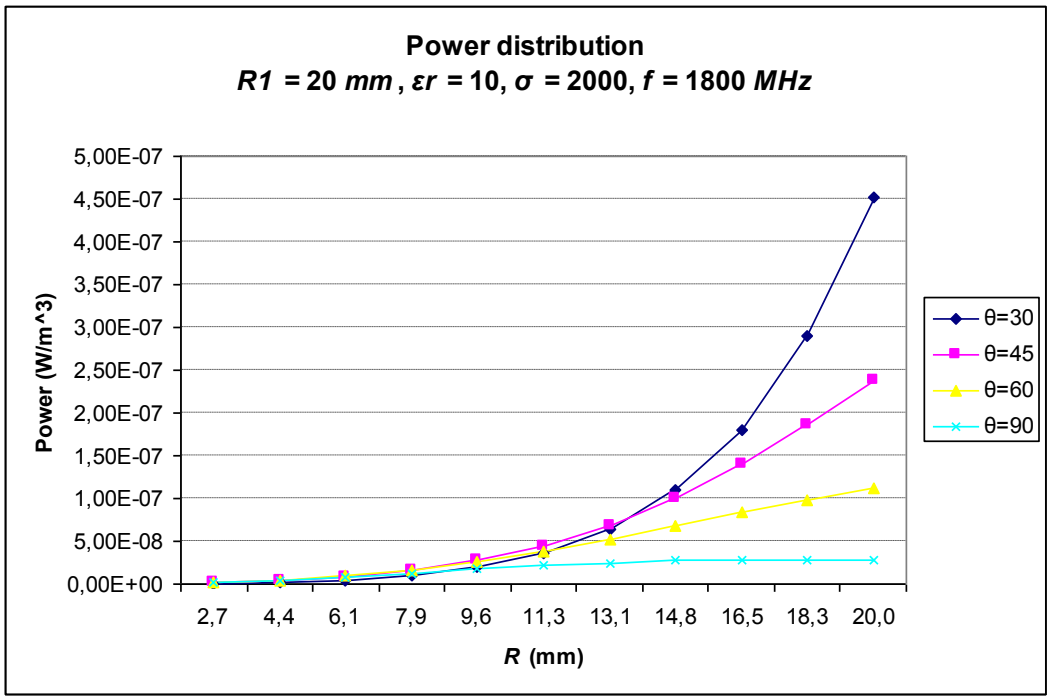

Figure 4.12: Heating potential at *f* =1800 *MHz*, R_{12}=3 *cm*, a_1=1 *cm*

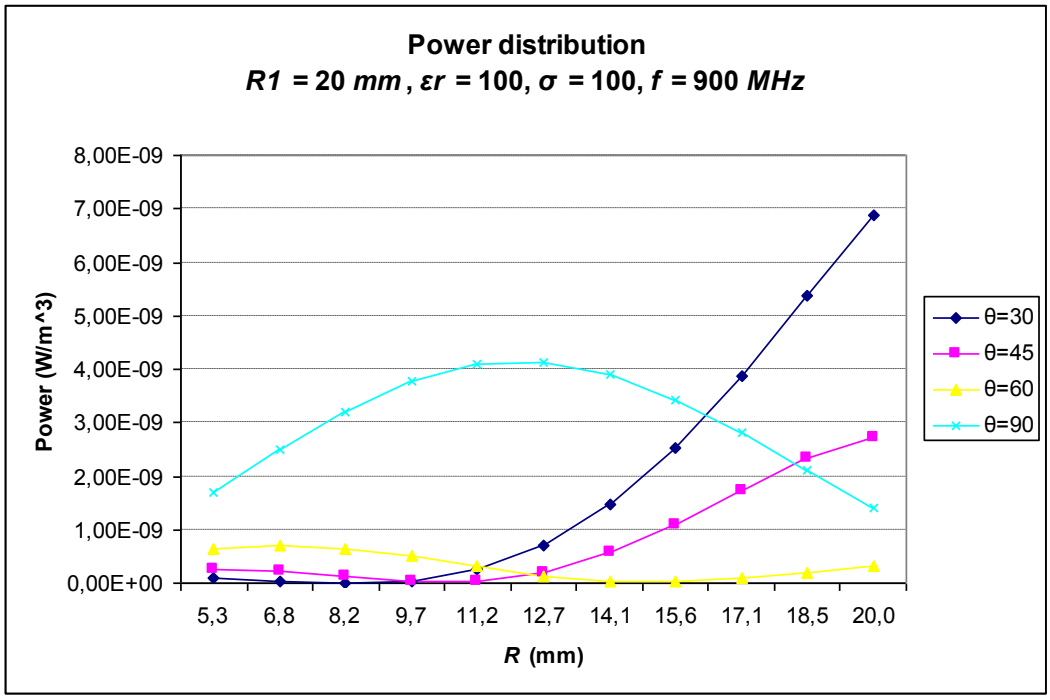

Figure 4.13: Heating potential at f =900 *MHz*, R_{12}=3 *cm*, a_1=1 *cm*

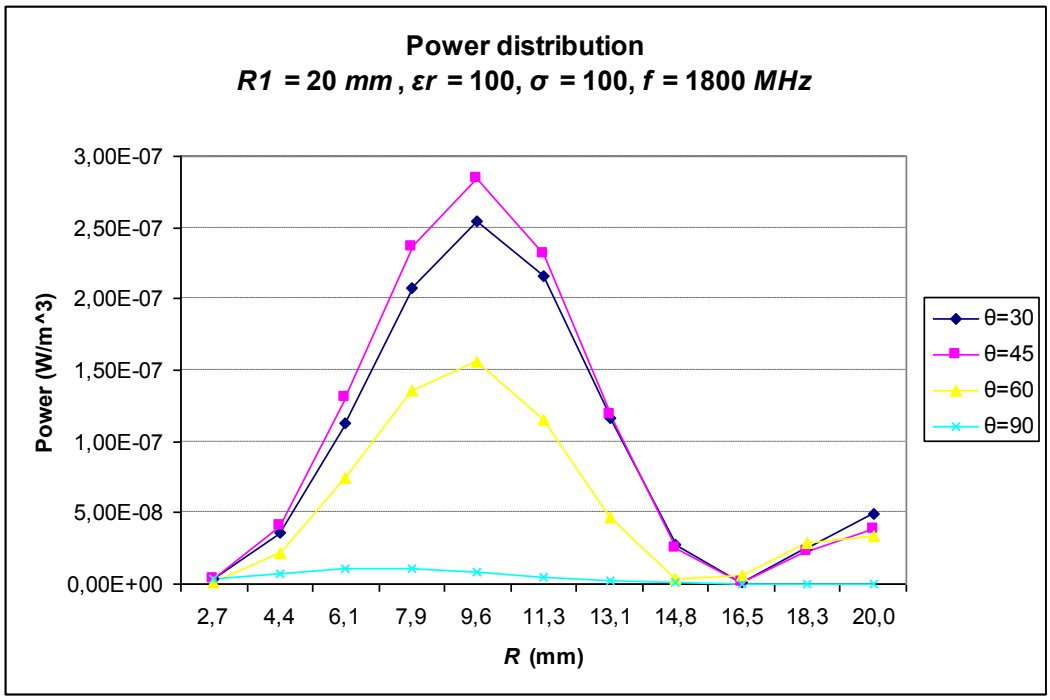

Figure 4.14: Heating potential at f =1800 *MHz*, R_{12}=3 *cm*, a_1=1 *cm*

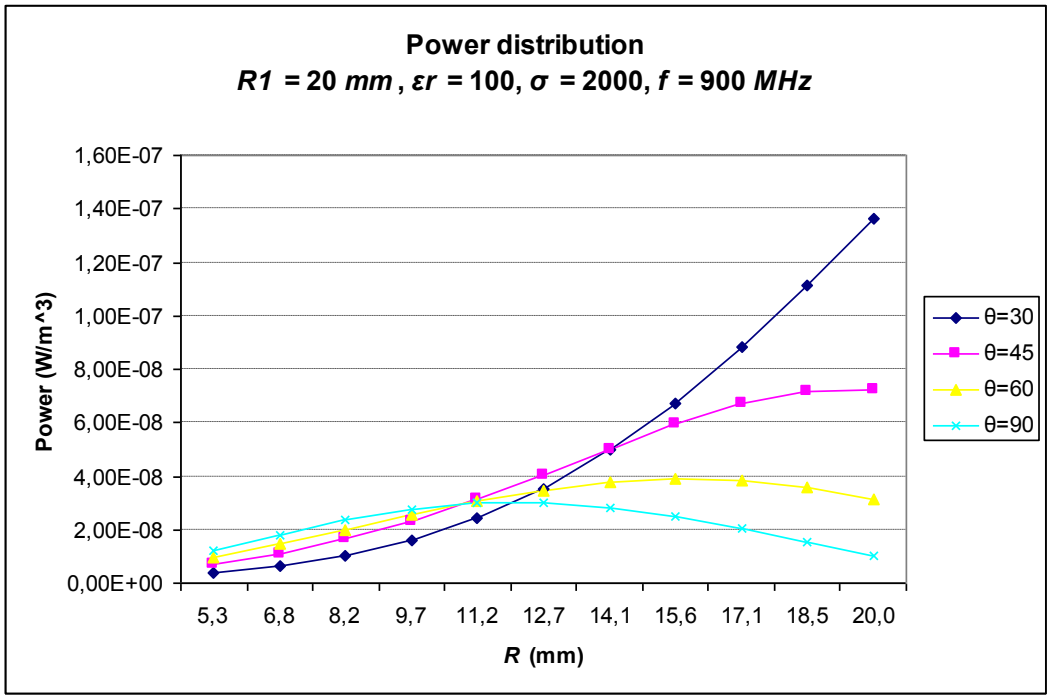

Figure 4.15: Heating potential at *f* =900 *MHz*, R_{12}=3 *cm*, a_1=1 *cm*

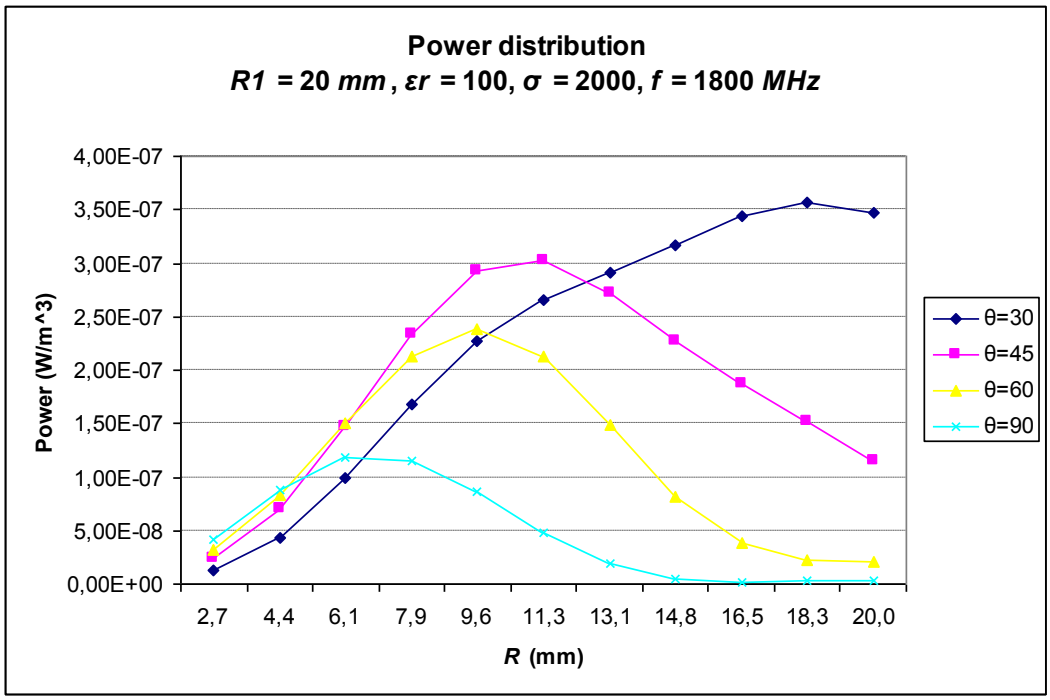

Figure 4.16: Heating potential at *f* =1800 *MHz*, R_{12}=3 *cm*, a_1=1 *cm*

Figures 4.17-4.20 show the variations of the heating potentials versus the conductivity of the dielectric material. As seen in these figures, heating potential proportionally increases as the conductivity increase. Heating potential does not vary versus ε_r, so these plots are not given.

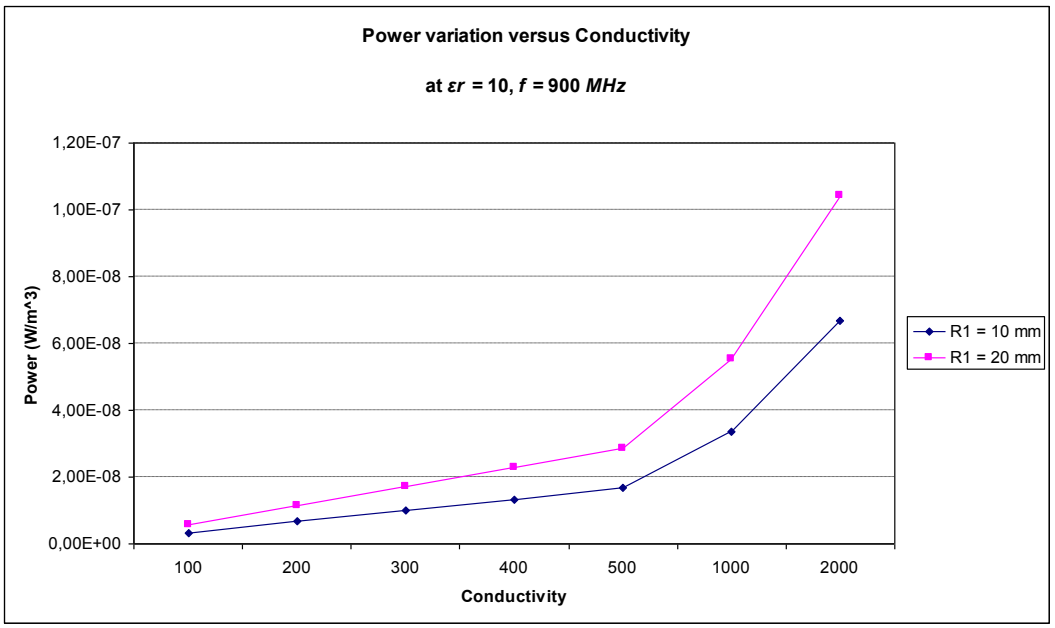

Figure 4.17: Power variation versus σ , at ε_r = 10, f = 900 *MHz*

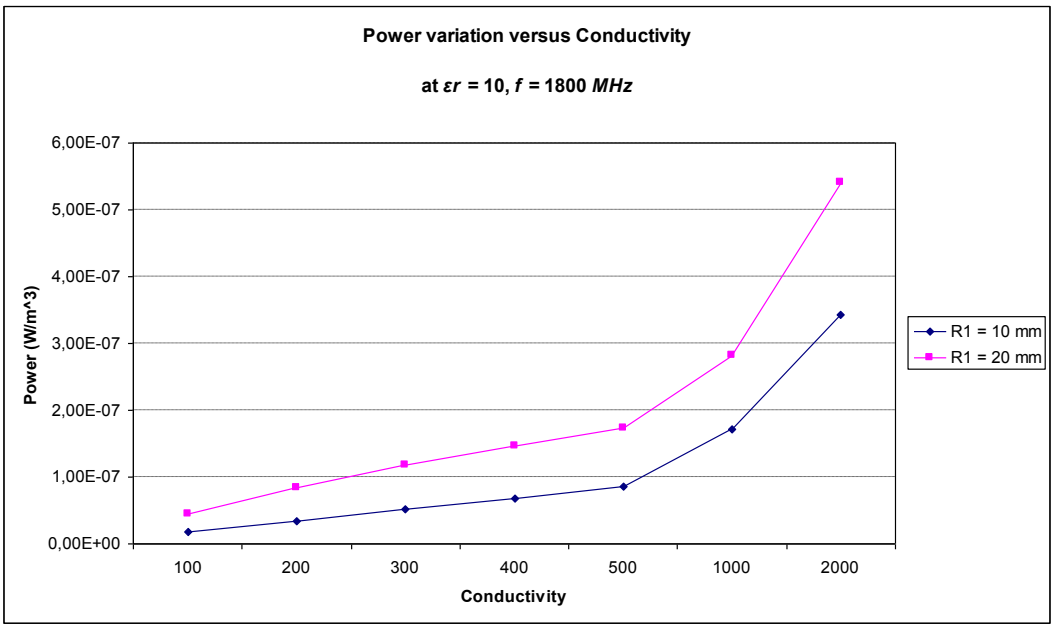

Figure 4.18: Power variation versus σ, at ε_r = 10, f = 1800 *MHz*

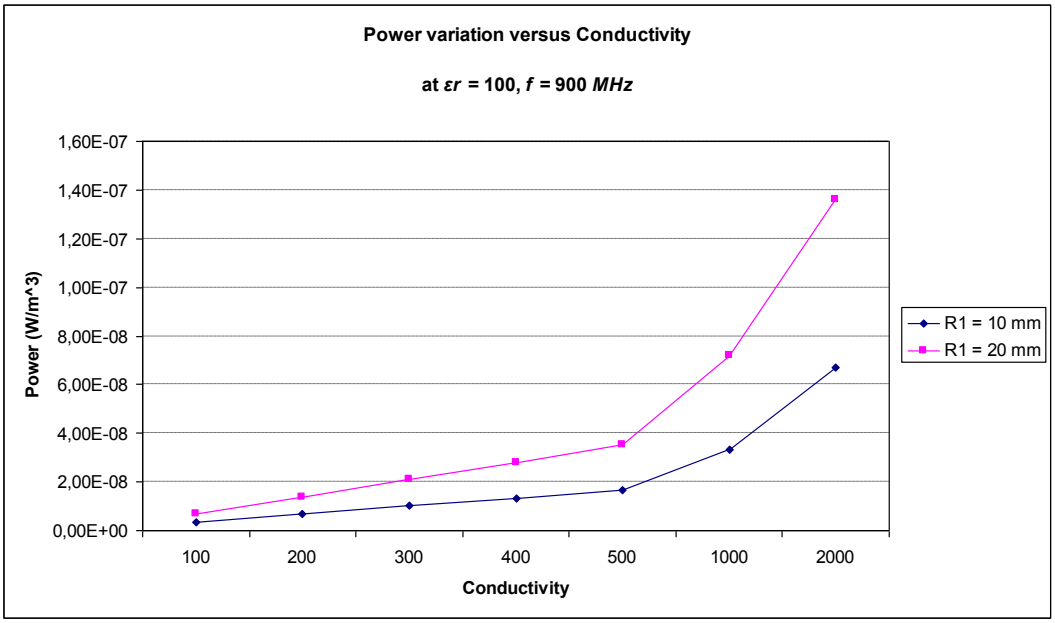

Figure 4.19: Power variation versus σ , at ε_r = 100, f = 900 *MHz*

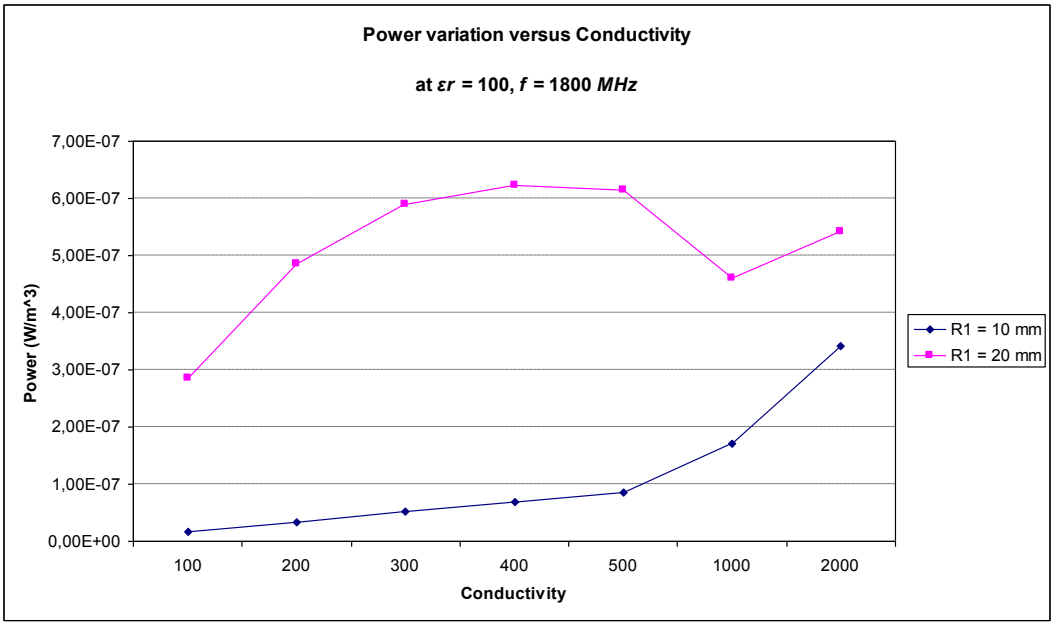

Figure 4.20: Power variation versus σ , at ε_r = 100, f = 1800 *MHz*

For a homogeneous spherical object that has 10 mm radius, the absorbed maximum power values are given in Tables 4.1-4.4.

Table 4.1: For ε_r = 10, σ = 100, R_{12}=2 *cm*, absorbed max. power values

	900 MHz	1800 MHz
θ	Max. Power (W/m^3)	Max. Power (W/m^3)
30^0	0,31E-08	0,15E-07
45^0	0,33E-08	0,17E-07
60^0	0,25E-08	0,14E-07
90^0	0,99E-09	0,59E-08

Table 4.2: For ε_r = 10, σ = 2000, R_{12}=2 *cm*, absorbed max. power values

	900 MHz	1800 MHz
θ	Max. Power (W/m^3)	Max. Power (W/m^3)
30^0	0,61E-07	0,30E-06
45^0	0,67E-07	0,34E-06
60^0	0,51E-07	0,27E-06
90^0	0,20E-07	0,12E-06

Table 4.3: For ε_r = 100, σ =100, R_{12}=2 *cm*, absorbed max. power values

	900 MHz	1800 MHz
θ	Max. Power (W/m^3)	Max. Power (W/m^3)
30^0	0,31E-08	0,15E-07
45^0	0,33E-08	0,17E-07
60^0	0,25E-08	0,14E-07
90^0	0,98E-09	0,59E-08

Table 4.4: For ε_r = 100, σ =2000, R_{12}=2 *cm*, absorbed max. power values

	900 MHz	1800 MHz
θ	Max. Power (W/m^3)	Max. Power (W/m^3)
30^0	0,61E-07	0,30E-06
45^0	0,67E-07	0,34E-06
60^0	0,51E-07	0,27E-06
90^0	0,20E-07	0,12E-06

For a homogeneous spherical object that has 20 mm radius, absorbed maximum power values are given in Tables 4.5-4.8.

Table 4.5: For ε_r = 10, σ = 100, R_{12}=3 *cm*, absorbed max. power values

	900 MHz	**1800 MHz**
θ	**Max. Power (W/m^3)**	**Max. Power (W/m^3)**
30^0	0,57E-08	0,44E-07
45^0	0,32E-08	0,35E-07
60^0	0,17E-08	0,26E-07
90^0	0,47E-09	0,17E-07

Table 4.6: For ε_r = 10, σ = 2000, R_{12}=3 *cm*, absorbed max. power values

	900 MHz	**1800 MHz**
θ	**Max. Power (W/m^3)**	**Max. Power (W/m^3)**
30^0	0,10E-06	0,54E-06
45^0	0,58E-07	0,34E-06
60^0	0,28E-07	0,18E-06
90^0	0,74E-08	0,58E-07

Table 4.7: For ε_r = 100, σ =100, R_{12}=3 *cm*, absorbed max. power values

	900 MHz	**1800 MHz**
θ	**Max. Power (W/m^3)**	**Max. Power (W/m^3)**
30^0	0,69E-08	0,26E-06
45^0	0,29E-08	0,29E-06
60^0	0,14E-08	0,16E-06
90^0	0,41E-08	0,10E-07

Table 4.8: For ε_r = 100, σ =2000, R_{12}=3 *cm*, absorbed max. power values

	900 MHz	**1800 MHz**
θ	**Max. Power (W/m^3)**	**Max. Power (W/m^3)**
30^0	0,14E-06	0,54E-06
45^0	0,73E-07	0,34E-06
60^0	0,39E-07	0,24E-06
90^0	0,30E-07	0,12E-06

CHAPTER 5

CONCLUSION

The heat distributions generated in human head are investigated at GSM frequencies of 900 MHz and 1800 MHz. Head is modelled by concentric spheres of brain, bone and skin. Complex dielectric structure of the concentric spheres are excited by a thin wire loop antenna.

For $ka_1 = 0{,}3$ constant, it is that seen the heat increases as we go from the center of the head to the outer regions, it reaches maximum at the area that join the brain and the bone, decreases at the bone and increases at the skin again. In the head model, it is that heat generally decreases as θ increases, maximum heat occurs at the center of the brain. When R_{12} distance increases, heat decreases and the maximum heat occurs for big θ. It is that seen the heat behavior pattern at 900 MHz is similar to 1800 MHz but heat level decreases at 1800 MHz. Also SAR values are presented in tables.

For $a_1 = 1\,cm$, heat level at 1800 MHz is higher than that of 900 MHz. Other heat behavior pattern is similar to $ka_1 = 0{,}3$ situtation. SAR values are presented in tables again. For above two situations, SAR values are lower than limits imposed by the standards.

To investigate the relation between the heat potential, permittivity and the conductivity, the results are obtained for any two spherical objects with 10 mm and 20 mm radius that are excited by a loop antenna located at 1 cm distance from the objects surface at 900 MHz and 1800 MHz.

For the object with 10 mm radius, maximum heat occurred at $\theta = 45^0$. Also it is observed that the heat level at 1800 MHz is higher than 900 MHz.

For the object with 20 mm radius, maximum heat occurred at $\theta = 30^0$ except f = 1800 *MHz*, $\varepsilon_r = 100, \sigma = 100$ situation. It is that seen the heat level at 1800 MHz is higher than 900 MHz.

It is concluded that the heating potential proportionally varies depending on the conductivity, however, the heating potential does not vary versus permittivity.

REFERENCES

[1] **Khalatbari, S.** et. al. (2006), *Calculating SAR in Two Models of the Human Head Exposed to Mobile Phones Radiations at 900 and 1800 MHz*, Proc. PIERS, 104-109.

[2] **Liu, F.** et. al. (2004), *Dyadic Green Function/MoM based Method for the Analysis of Electromagnetic Fields inside a Lossy, Multilayered Spherical Head Phantom Excited By RF Coil*, Proc. Intl. Soc. Mag. Med. 11.

[3] **Kim, J., Rahmat-Samii, Y.** (2005), *On the Applicability of Simplified Spherical Human Heads for Implanted Antennas in Biomedical Communications*, Electromagnetics, 25:491-511.

[4] **Reyhani, S.M.S., Ludwig, S.A.** (2006), *An Implanted Spherical Head Model Exposed to Electromagnetic Fields at a Mobile Communication Frequency*, IEEE Transactions on Biomedical Engineering, Vol. 53, No. 10.

[5] **Chen, H.Y., Wang, H.H.** (1994), *Current and SAR Induced in a Human Head Model by the Electromagnetic Fields Irradiated from a Cellular Phone*, IEEE Transactions on Microwave Theory and Techniques, Vol. 42, No. 12.

[6] **Nikita, K.S.** et. al. (2000), *Analysis of the Interaction Between a Layered Spherical Human Head Model and a Finite-Length Dipole*, IEEE Transactions on Microwave Theory and Techniques, Vol. 48, No. 11.

[7] **Skaropoulos, N.C., Ioannidou, M.P., Chrissoulidis, D.P.** (1996), *Induced EM Field in a Layered Eccentric Spheres Model of the Head: Plane-Wave and Localized Source Exposure*, IEEE Transactions on Microwave Theory and Techniques, Vol. 44, No. 10.

[8] **Eds. Vecchia, P.** et. al. (2009), *Exposure to High Frequency Electromagnetic Fields, Biological Effects and Health Consequences (100 kHz-300 GHz), International Commission on Non-Ionizing Radiation Protection*, ICNIRP, http://www.icnirp.de/documents/RFReview.pdf.

[9] **Cleveland, Robert F., Ulcek Jerry L.** (1999), *Questions and Answers about Biological Effects and Potential Hazards of Radiofrequency Electromagnetic Fields*, Federal Communications Commission Office of Engineering and Technology.

[10] **Goldsworthy, A.** (2007), *The Dangers of Electromagnetic Smog*, Imperial College, London.

[11] **Scientific Comittee On Emerging And Newly Identified Health Risks (SCENIHR)**, (2006), *Possible effects of Electromagnetic Fields (EMF) on Human Health*.

[12] **Kramarenko, A.V., Uner, T.** (2003), *Effects of High-Frequency Electromagnetic Fields On Human EEG: A Brain Mapping Study*, Intern. J. Neuroscience, 113:1007-1019.

[13] **Kumar, N., Kumar, G.** *Biological Effects of Electromagnetic Radiation*, Wilcom Technologies Pvt. Ltd.

[14] **Weinberger, Z., Richter, E. D.** (2002), *Cellular Telephones and Effects on the Brain: The Head as an Antenna and Brain Tissue as a Radio Receiver*, Elseiver Science Ltd.

[15] **Marino, A.A., Nilsen, E., Frilot, C.** (2003), *Nonlinear Changes in Brain Activity Due to Cell Phone Radiation*, Bioelectromagnetics 24:339-346.

[16] **Lin, J.C.** (2003), *Cataracts and Cell-Phone Radiation*, IEEE Antennas and Propogation Magazine, Vol. 45. No. 1.

[17] **DeMarco, S.C.** et al. (2003), *Computed SAR and Thermal Elevation in a 0.25-mm 2-D Model of the Human Eye and Head in Response to an Implanted Retinal Stimulator*, IEEE Transactions on Antennas and Propogation, Vol. 51, No. 9.

[18] **Fujino, T., Hirata, A., Shiozawa, T.** (2003), *Evaluation of Induced SAR in the Human Body due to EM Waves Emitted from a Dipole Antenna at 400 MHz Band*, IEEE 0-7803-8197-1/03.

[19] **Paker, S., Sevgi, Levent.** (1998), *FDTD Evaluation of the SAR Distribution in a Human Head Near a Mobile Cellular Phone*, TÜBİTAK, Elektrik, Vol. 6, No.3.

[20] **Lin, J.C.** *Health Aspects of Wireless Communication: Mobile Telephone Radiation and the Exposure of Children*, Mobile Computing and Communications Review, Volume 7, Number 1.

[21] **Hızal, A., Baykal, Y. K.** (1978), *Heat Potential Distribution in an Inhomogeneous Spherical Model of a Cranial Structure Exposed to Microwaves Due to Loop or Dipole Antennas,* IEEE Trans. Microwave Theory and Techniques, MTT-26, 607-612.

[22] **Baykal, Y. K.** (1977), *Heat Distribution in an Inhomogeneous Model of Head Exposed to Microwave Radiation Due to Loop or Dipole Antenna Excitations,* published M.S.C. thesis, METU, Ankara.

[23] **Mahapatra, S., Dey, T. K.** *Effect of Electromagnetic Radiation On Bio-objects.*

[24] **Turgut, G., Yazgan, E.** *Canlılar ve Haberleşme Sistemlerinde Elektromanyetik Kirlilik ve İlgili Standartlar*, Hacettepe University.

[25] **TÜBİTAK-BİLTEN**, (2001), *Elektromanyetik Dalgalar ve İnsan Sağlığı Sıkça Sorulan Sorular ve Yanıtları*.

[26] http://www.tgm.gov.tr/doc/10khz_60ghz.doc (Access 05.09.2010)

[27] http://www.sarvalues.com (Access 05.09.2010)

[28] http://www.gnrk.gazi.edu.tr/sar.htm (Access 05.09.2010)

[29] http://www.ece.msstate.edu/~donohoe/ece3323antennas.pdf (Access 06.09.2010)

APPENDIX A

A.1 Calculation of SAR

Complex dielectric coefficient for a lossy dielectric material is written as

$$\in = \in_0 (\in_r^{'} - j \in_r^{*}) \qquad (A.1.1)$$

Conductivity for same material is found

$$\sigma = \omega_0 \in_0 \in^{*} \qquad (A.1.2)$$

If this environment is in a electric field, conductivity can be written as

$$\bar{J} = \sigma \bar{E} \qquad (A.1.3)$$

If this environment is defined for a living thing, electromagnetic field is absorbed by living thing. Absorbed energy by a living thing can be calculated as

$$SAR = \frac{\sigma}{2\rho} \int_V E^2 dV \qquad (A.1.4)$$

Here, σ: conductivity (S/m)

ρ: mass density (kg/m^3)

E: electric field (V/m)

define [24].

A.2 Electric Field of Loop Antenna

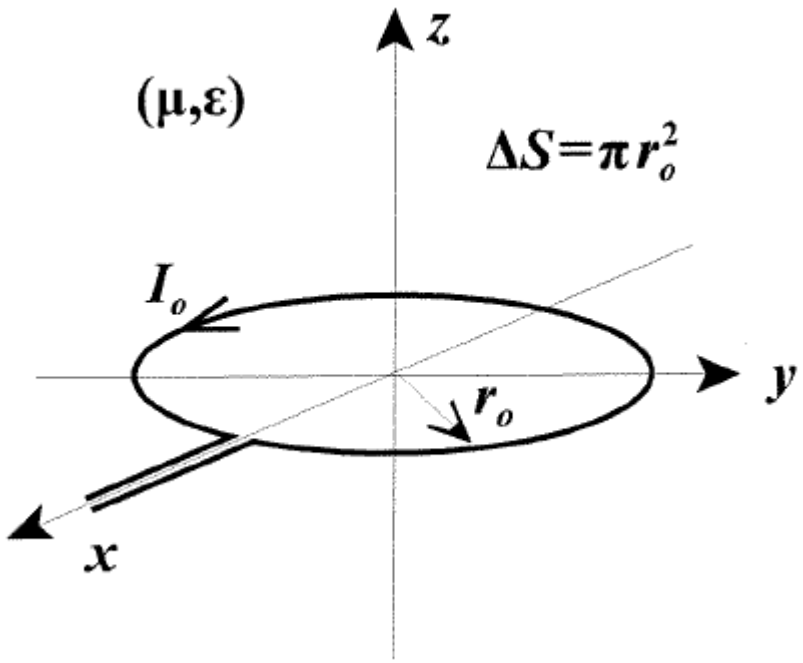

Figure A.2.1: Small loop antenna

Small loop radiated fields.

$$\tilde{H}_r = jk^3 \frac{I_0 \Delta S}{2\pi} \cos\theta \left[\frac{1}{(kR)^2} - \frac{j}{(kR)^3} \right] e^{-jkR} \qquad (A.2.1)$$

$$\tilde{H}_\theta = jk^3 \frac{I_0 \Delta S}{4\pi} \sin\theta \left[\frac{j}{kR} + \frac{1}{(kR)^2} - \frac{j}{(kR)^3} \right] e^{-jkR} \qquad (A.2.2)$$

$$\tilde{E}_\phi = -j\eta k^3 \frac{I_0 \Delta S}{4\pi} \sin\theta \left(\frac{j}{kR} + \frac{1}{(kR)^2} \right) e^{-jkR} \qquad (A.2.3)$$

The terms in the radiated field expressions which vary as $1/(kR)$ represent the small loop far field.

Small loop far fields

$$\tilde{H}_\theta \approx -k^2 \frac{I_0 \Delta S}{4\pi R} \sin\theta \, e^{-jkR} \qquad (A.2.4)$$

$$\tilde{E}_\phi \approx \eta k^2 \frac{I_0 \Delta S}{4\pi R} \sin\theta \, e^{-jkR} \qquad (A.2.5)$$

[29].

APPENDIX B

B.1 Limit Values in Turkey

Table B.1.1: Limit values for uncontrolled exposure in Turkey [25]

Frequency	**900 MHz**		**1800 MHz**	
	Limit value for a device	Total limit value of environment	Limit value for a device	Total limit value of environment
Electric Field Strength	10,23 V/m	41,25 V/m	14,47 V/m	58,34 V/m
Magnetic Field Strength	0,027 A/m	0,111 A/m	0,038 A/m	0,157 A/m
Power Density	0,28 W/m^2	4,5 W/m^2	0,56 W/m^2	9,0 W/m^2

Table B.1.2: Limit values for controlled exposure [25]

Limit Values for 900 MHz	**ICNIRP**	**IEEE/FCC**
Electric Field Strength	90,0 V/m	-
Magnetic Field Strength	0,24 A/m	-
Power Density	22,5	30,0
Limit Values for 1800 MHz	**ICNIRP**	**IEEE/FCC**
Electric Field Strength	127,28 V/m	-
Magnetic Field Strength	0,34 A/m	-
Power Density	45,0 W/m^2	50,0 W/m^2

ICNIRP limit values that applied in European countries are to be taken consideration, electric field strength limit value that correspond to ¼ of standart value has been accepted as basic criterion in regulations [26].

B.2 SAR Values of Cell Phones

Table B.2.1: The ten highest radiating cell phones (Europe) [27]

Manufacturer	**Model**	**SAR** (W/kg)
Sony Ericsson	T650	1,80
Sony Ericsson	W880i	1,45
Nokia	E51	1,40
Sony Ericsson	W950i	1,35
Sony Ericsson	Z610i	1,32
Sony Ericsson	K810i	1,31
Sony Ericsson	W610i	1,31
Sony Ericsson	W660i	1,27
Sony Ericsson	K550i	1,25
LG+Nokia	KU250+N5700	1,24

Table B.2.2: The ten lowest radiating cell phones (Europe) [27]
(Max exposure 10 Wkg in 10 Grams of Tissue)

Manufacturer	**Model**	**SAR** (W/kg)
Samsung	F210	0,20
Nokia	6267	0,31
Emporia	Life	0,37
HTC	TYTN11	0,38
LG	KE970 Shine	0,43
LG	KU970	0,43
Nokia	6290	0,47
Samsung	U600	0,48
Nokia	8800i	0,50
LG	KG130	0,52

0,1 (W/kg) SAR value is adviced for cell phones in WHO EMF Project by performed WHO (World Health Organization) since 1996 [29].

APPENDIX C

CURRICULUM VITAE

PERSONAL INFORMATION

Surname, name: Türk, Afşar
Nationality: Turkish (TC)
Date and Place of Birth: 19 October 1976, İzmir
Marital Status: Single
Phone: +90 532 325 82 34
email: afsarturk@gmail.com

EDUCATION

Degree	Institution	Year of Graduation
MS	Ahmet Yesevi University, Computer Engineering	2006
BS	Anadolu University, Aviation Electrical and Electronics	1999
High School	Aydın Techinal High School, Department of Electronics	1993

WORK EXPERIENCE

Year	Place	Enrollment
2010 March-Present	General Directorate of TEDAŞ	Chief
2000 September-2010 March	General Directorate of TEDAŞ	Programmer
1997 August	Air Alfa Airlines	Intern

FOREIGN LANGUAGES

English.

HOBBIES

Literature, Music, Movies, Swimming, Football.